# HIGHWAY RESEARCH RECORD

## Number 111

# Soil Drainage and Other Soil-Water Phenomena

## 4 Reports

Presented at the
44th ANNUAL MEETING
January 11-15, 1965

SUBJECT CLASSIFICATION
63 Mechanics (Earth Mass)
64 Soil Science

HIGHWAY RESEARCH BOARD
of the
Division of Engineering and Industrial Research
National Academy of Sciences—National Research Council
Washington, D. C.
1966

# *Department of Soils, Geology and Foundations*

Eldon J. Yoder, Chairman
Joint Highway Research Project
Purdue University, Lafayette, Indiana

DIVISION B

H. Bolton Seed, Chairman
Department of Civil Engineering
University of California, Berkeley

## COMMITTEE ON STRENGTH AND DEFORMATION CHARACTERISTICS OF PAVEMENT SECTIONS

(As of December 31, 1964)

Carl L. Monismith, Chairman
University of California, Berkeley

E. S. Barber, Consulting Engineer, Soil Mechanics and Foundations, Arlington, Virginia
Bonner S. Coffman, Department of Civil Engineering, Ohio State University, Columbus
B. E. Colley, Manager, Paving Development Section, Portland Cement Association, Skokie, Illinois
F. N. Finn, Chief Engineer, Materials Research and Development, Oakland, California
Raymond Forsyth, Materials and Research Department, California Division of Highways, Sacramento
W. S. Housel, University of Michigan, Ann Arbor
W. Ronald Hudson, Department of Civil Engineering, University of Texas, Austin
R. L. Kondner, Department of Civil Engineering, Northwestern University, Evanston, Illinois
H. G. Larew, Department of Civil Engineering, University of Virginia, Charlottesville
T. F. McMahon, U. S. Bureau of Public Roads, Washington, D. C.
B. P. Shields, Research Council of Alberta, Edmonton, Alberta, Canada
Eugene L. Skok, Jr., Department of Civil Engineering, University of Minnesota, Minneapolis
J. E. Stephens, Professor of Civil Engineering, University of Connecticut, Storrs
Aleksandar Vesic, Department of Civil Engineering, Georgia Institute of Technology, Atlanta

## COMMITTEE ON SUBSURFACE DRAINAGE

(As of December 31, 1964)

Harry R. Cedergren, Chairman
State Department of Water Resources
Sacramento, California

E. S. Barber, Consulting Engineer, Soil Mechanics and Foundations, Arlington, Virginia
K. J. Boedecker, Jr., Richmond, Virginia
Kenneth S. Eff, Chief, Hydraulic Section, Civil Engineering Branch, Office, Chief of Engineers, Department of the Army, Washington, D. C.
A. D. Hirsch, Materials and Research Department, California Division of Highways, Sacramento
Ronald D. Hughes, Research Engineer, Highway Research Laboratory, University of Kentucky, Lexington

Carl F. Izzard, Chief, Hydraulic Research Division, Office of Research and Development, U. S. Bureau of Public Roads, Washington, D. C.
Philip Keene, Engineer of Soils and Foundations, Connecticut State Highway Department, Wethersfield
W. R. Lovering, District Engineer, The Asphalt Institute, Sacramento, California
George W. McAlpin, Deputy Chief Engineer (Research), New York State Department of Public Works, Technical Services Subdivision, Albany
John D. McNeal, Research Engineer, State Highway Commission of Kansas, Topeka
Alfred W. Maner, Staff Engineer, The Asphalt Institute, University of Maryland, College Park
Carl I. Olsen, Site Planning Division, Architectural-Structural Service, Office, Assistant Administrator for Construction, Veterans Administration, Washington, D. C.
G. G. Parker, Branch of General Hydrology, U. S. Geological Survey, Denver Federal Center, Denver, Colorado
O. J. Porter, Managing Partner, Porter, O'Brien and Armstrong, Newark, New Jersey
John M. Robertson, Manager, Drainage and Allied Products Sales, Metal Products Division, Armco Steel Corporation, Middletown, Ohio
E. P. Sellner, Manager, Water Resources Bureau, Portland Cement Association, Chicago, Illinois
W. G. Shockley, Chief, Mobility and Environmental Division, Waterways Experiment Station, Vicksburg, Mississippi
Rockwell Smith, Research Engineer - Roadway, Association of American Railroads, Chicago, Illinois
W. T. Spencer, Soils Engineer, Materials and Tests, Indiana State Highway Commission, Indianapolis
Hans F. Winterkorn. Professor of Civil Engineering, Princeton University, Princeton, New Jersey

## DIVISION C

O. L. Lund, Chairman
Assistant Engineer of Materials and Tests
Nebraska Department of Roads, Lincoln

## COMMITTEE ON PHYSICO-CHEMICAL PHENOMENA IN SOILS

(As of December 31, 1964)

Hans F. Winterkorn, Chairman
Professor of Civil Engineering
Princeton University, Princeton, New Jersey

Gail C. Blomquist, School of Civil Engineering, Michigan State University, East Lansing
James H. Havens, Director of Research, Kentucky Department of Highways, Lexington
J. B. Hemwall, The Dow Chemical Company, Chemicals Laboratory, Midland, Michigan
Earl B. Kinter, U. S. Bureau of Public Roads, Washington, D. C.
Joakim G. Laguros, Department of Civil Engineering, University of Oklahoma, Norman
Philip F. Low, Department of Agronomy, Purdue University, Lafayette, Indiana
R. C. Mainfort, Michigan State Highway Department, Lansing
Edward Penner, Division of Building Research, National Research Council of Canada, Ottawa
Elmer A. Rosauer, Engineering Experiment Station, Iowa State University, Ames
J. B. Sheeler, Associate Professor of Civil Engineering, Engineering Experiment Station, Iowa State University, Ames
Mehmet A. Sherif, Department of Civil Engineering, University of Washington, Seattle
F. L. D. Wooltorton, Truffles, Pigbush Lane, Loxwood, Billingshurst, Sussex, England

# Foreword

The forces required to move water through soils differ greatly, depending on soil type, soil state, and the manner in which the soils retain and thus restrict movement. Water permeates freely in sands and gravels under the natural force of gravity. Water movement in clays in nature requires very high suction forces, of the magnitude produced by evaporation processes.

In 1808, Reuss discovered that an electric force field in the form of a direct current applied to an electrode in a clay soil can be made to force water through that soil to another electrode some distance away. As knowledge of this process, called electroosmosis, has increased, several investigators have attempted to formulate the interrelationships between soil type, soil state, water content, and the electric force field to make them more understandable and more applicable. Esrig and Majtenyi have shown that these complex relationships can be arranged in a relatively simple equation that provides a better understanding of the electroosmosis phenomenon.

The great forces that clayey soils exert in attracting, moving and holding moisture have long been termed "suction" by soil scientists and "negative pore pressure" by engineers. Several methods have been employed to measure this force. Each method has its optimum range and its other special features. Kassif and Globinsky have constructed an apparatus that has the advantage of continuously measuring suctions in a single operation and is applicable to a wide range of soil textures. The significance of better means for measurement lies in its potential usefulness in predicting trends in soil shrinkage or swelling under areas subjected to external loads.

Distortion of pavements due to swelling or shrinking of the underlying soils has been, and may long be, a source of difficult and costly problems to engineers who design, build and operate highway and airfield pavements. The problems are more acute in arid and semiarid regions where soils are either being wetted or dried. Kassif and Wiseman have concerned themselves principally with swelling and shrinkage near the edges of a runway pavement where they recorded heaves up to 20 cm (about 8 in.). They have measured the developed suction (negative pore pressures) in the soil, the movements of pavement at edges, and variations in moisture content in the clay shoulders of the runway. Their paper shows the benefits derived from careful design and proper placement of a subsurface drainage system near the edges of the pavement.

Numerous attempts have been made to study the cause and effect of pumping of concrete pavements by means of laboratory models. Stowe, Handy and Fero review the results of previous attempts and construct a model with simulated jointed slabs and wheel loads traveling across the jointed slabs. The model scaled dimensionally and in loading yielded data in terms of deflection and cohesion vs repetitions of load. The new data add to the storehouse of knowledge that engineers now have available for their use in designing pavements to prevent the occurrence of pumping.

# Contents

# Control of Moisture and Volume Changes in Clay Subgrades by Subdrainage

G. KASSIFF and G. WISEMAN
Senior Lecturers, Faculty of Civil Engineering, Israel Institute of Technology

Observations of the vertical heave at the edge of a runway pavement and moisture variations in the clay subgrade as affected by the subdrainage system are presented. The paper also reports on a model study of the effect of two different filter materials on the drying of the clay subgrade near the subdrainage under different surfacing conditions.

It was found that the subdrainage system has a definite beneficial effect on the moisture distributions in the clay. By removing free water which penetrates cracks, it helps in maintaining a low range of moisture variations between summer and winter and thus inhibits large movement at the edge of the pavement.

The selection of the filter material should be governed mainly by moisture variation considerations. It is desirable to use a fine permeable material for the subdrainage system because such a material would tend to serve as a moisture reservoir for the clay during the drying period and act as a capillary cut-off against drying out of the clay underneath the pavement.

•SHOULDERS OF ROADS and runways built on expansive clay subgrades in Israel are usually left unsurfaced. As a result they are highly susceptible to climatic changes. They heave vertically and move laterally on wetting, and crack on drying. Thus, moisture tends to penetrate laterally under the edge of the pavement, causing volume changes in the clay subgrade and differential movement accompanied by cracking within the pavement itself. Because of low groundwater table, drainage facilities usually consist only of open ditches to remove surface runoff. Many engineers consider subsurface drainage unnecessary for fat clays.

In recent years, however, clay shoulders construction, particularly of runways, has incorporated properly designed subsurface systems to drain the base course. The drainage system is usually composed of an open-joint drain surrounded by fine crushed stones, as a filter material, buried at a shallow depth. In many cases, a narrow strip of the shoulders overlying and adjacent to the subdrainage system was covered with a cheap surfacing to protect the edge of the pavement.

Engineers who have worked with highways and runways have found that even for clay subgrades in semiarid climates the removal of subsurface water is often an important problem. The clay, despite being impervious when intact, develops vertical and horizontal cracking during the dry season, which makes it very pervious at the beginning of the winter rains. Movement observations of a pavement with covered shoulders indicated that the availability of a subdrainage system affects the moisture regime in the clay subgrade under both the pavement and the shoulders.

In the case of unsurfaced shoulders, drying of the clay plays a significant role in the moisture regime at the vicinity of the pavement edge. A relatively deep subdrainage system may help reduce moisture variations if fine sand is used as a filter material.

---

Paper sponsored by Committee on Subsurface Drainage.

At the start of the dry season the capillary water held in the sand helps to maintain the adjacent clay in a moist state. When capillary water is no longer available, the dry fine sand acts as a cutoff to further drying of the clay subgrade under the pavement.

This paper deals with observations of movements and moisture variations in clay subgrades of runways as affected by the subdrainage system. It also discusses a model study (1) of the effect of two different filter materials on the drying of the clay subgrade under different surfacing conditions.

## FIELD MOVEMENT OBSERVATIONS

Extensive field observations (2) of the behavior of a runway built on an expansive clay subgrade have been carried out since completion of the construction during the summer of 1956. The runway pavement was of the flexible type, with asphalt seal-coated granular shoulders extending 3.0 m on each side. No groundwater was encountered in borings of up to 15 m deep.

Surface water drainage was provided by sloping the shoulders on either side of the runway toward open ditches located at 45 m from the edge of the pavement. Base course and shoulder seepage subdrainage was also provided at both sides of the pavement, with the exception of 100 m on one side of the runway. The subdrainage system (Fig. 1) consisted of open-joint pipe laid in the bottom of an excavated trench located at the edge of the covered shoulders and backfilled with a filter of fine crushed stone to the level of the base course. The omission of the subdrainage system on one side

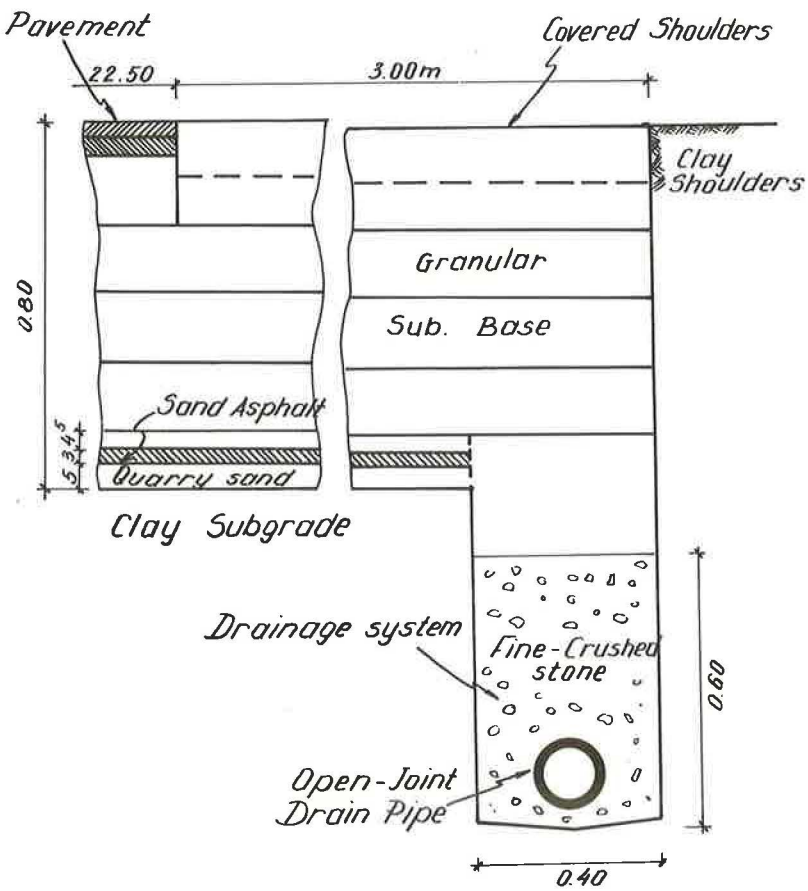


Figure 1. Section through pavement, shoulder and subdrainage system.

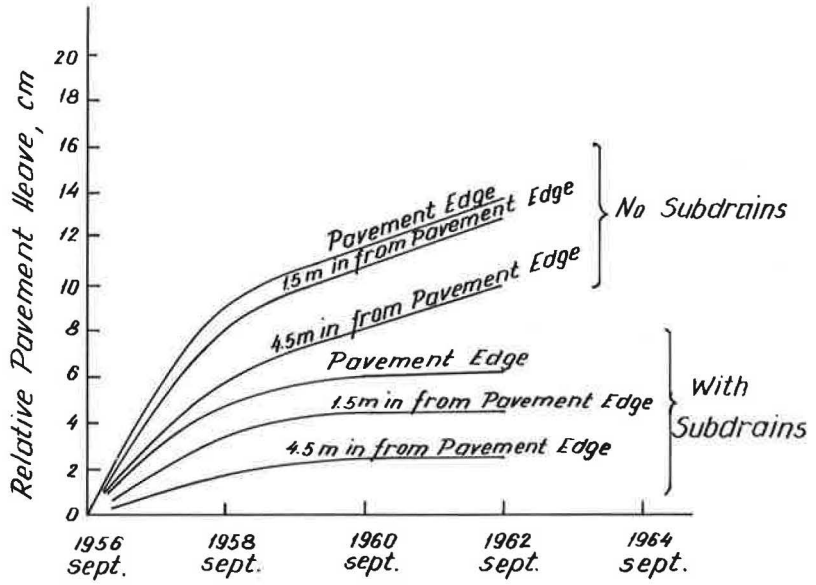


Figure 2. Movement of edge of pavement with and without subdrainage system.

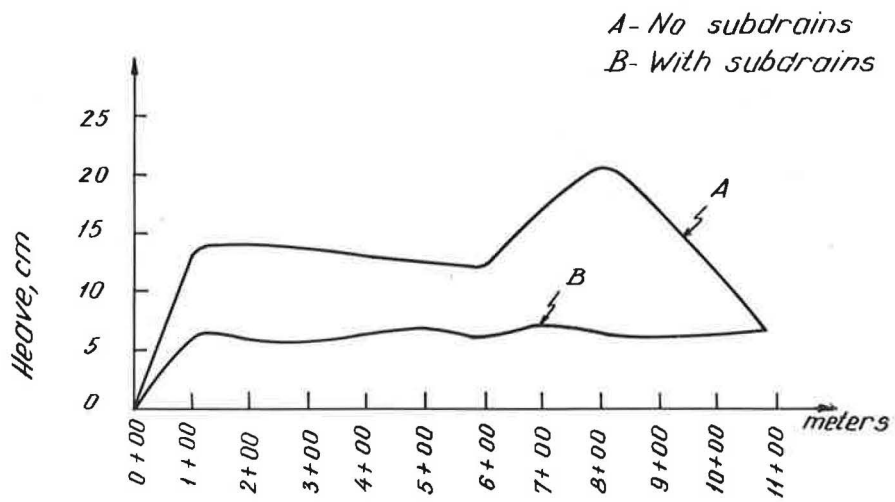


Figure 3. Longitudinal section of pavement showing heave of pavement edges.

of the pavement along the 100-m stretch provided a valuable opportunity for comparison of the effect of the system on movements of the pavement edges.

Level surveys of the vertical movements of the pavement with respect to a bench mark 11 m deep were made at the end of the summer for several years. The bench mark was protected by a pipe sleeve to isolate it from the upper soil movements. There was a general heave of the pavement. The results of the observations presented in Figures 2 and 3, however, are confined to the pavement center and therefore do not include the overall heave of the covered area. Figure 2 shows the accumulation of heave with time (1956-1962) at the sides of the pavement both with and without the subdrains, based on the averaging of 10 sections. A difference in heave of about 8 cm between the 2 sides of the pavement is shown. The side of the pavement with the subdrains, in addition to heaving less, showed less distortion of cross-section than the

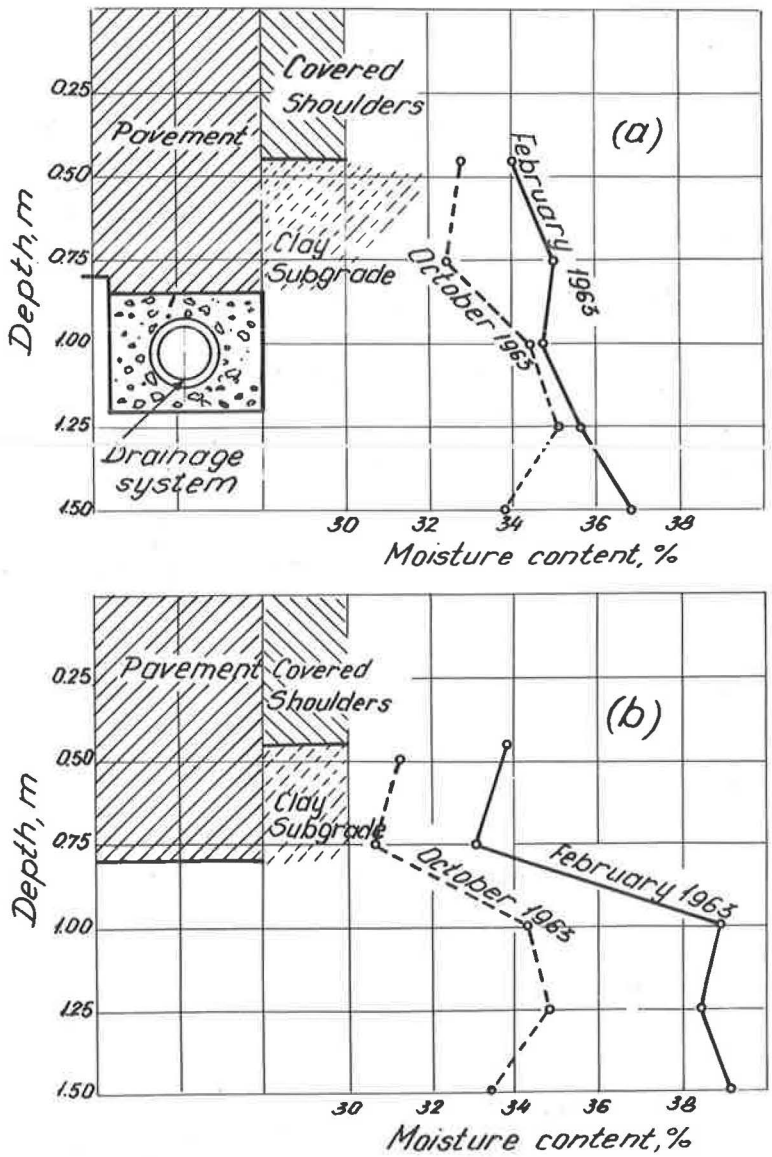


Figure 4. Moisture variations in clay shoulders of runway: (a) adjacent to drainage system, (b) without drainage facilities.

side without the subdrains. Whereas the side of the pavement with subdrains achieved a stable condition 4 yr after construction, the side without subdrains was still heaving 6 yr after construction.

Figure 3 shows the heave of the pavement edges on both sides of the 100-m stretch of the runway in longitudinal direction. The benefit of the subdrains may be easily observed from this figure. The intersection points between lines A and B represent heave at cross-sections at the beginning and the end of the 100-m stretch of runway which had subdrains on both sides.

## FIELD OBSERVATIONS OF MOISTURE PROFILES

Moisture distributions at the end of the wet and dry seasons, underneath covered-clay shoulders of a taxiway located at the same site where the vertical heave was measured, are shown in Figure 4. Figure 4a shows the distributions adjacent to the shoulder with a subdrainage system, and Figure 4b shows the distributions for the shoulder without the system. The range of moisture variation between summer and winter in the clay adjacent to the drainage system amounts to a maximum of 2.5 percent, whereas the same range for the other shoulder amounts to as much as 6 percent. These differences are significant by themselves, as they determine the amount of heave, but they served mainly for comparison with the moisture variations measured in the laboratory models.

These figures show that moisture conditions in the clay without the drainage, as compared with the other shoulder, were wetter at the end of the winter, whereas conditions at the end of the summer were essentially the same. The drainage system apparently helped to remove free water which penetrated the surface cracks in the shoulder and kept the moisture distribution within a close range of the summer profile. On the other hand, where no subdrainage facility was provided the water which penetrated the cracks caused a larger increase in the moisture range through saturation of the clay subgrade.

No measurements of the amount of water drained were made during these observations, but there was visual evidence of significant flow through the outlets, particularly during the initial period of the wet season.

## PURPOSE AND SCOPE OF MODEL STUDY

The specific purpose of the study was to determine the effect of various filter materials on the moisture distribution in the clay, particularly for exposed shoulders under drying conditions.

The study included models of moisture variations in a clay layer over-lying various filter materials, i.e., simulations of the clay in the vicinity of the drainage system. The following combinations were selected: (a) exposed clay on top of a fine dune sand; (b) exposed clay on top of a coarse crushed stone; and (c) covered clay on top of the filter materials as in a and b. The cover used consisted of 1-cm thick sand-asphalt layer.

The filter materials selected for this study represent a range of materials which, from a filter-criteria viewpoint, are considered adequate both to prevent migration of fines into the drainage system and to remove seepage quickly.

## DESCRIPTION OF SOILS STUDIED

The clay represents typical expansive clays in Israel. It is highly plastic (liquid limit (L. L.) = 65-80, plasticity index (P. I.) = 40-55, shrinkage limit (S. L.) = 8.5-11) and exhibits severe swelling properties. The dominant clay mineral is smectite (montmorillonite). The clay was sampled from the airfield in which the various measurements were made.

The dune sand is a fine, uniformly graded sand, with a 50 percent size of 0.15 mm and a maximum size of 0.5 to 0.8 mm. The saturated permeability of the sand is about $10^{-2}$ cm/sec. The coarse crushed stone originates from a limestone. It has a uniform gradation with a maximum size of 30 mm and 50 percent size of 15 mm.

## DESCRIPTION OF MODEL STUDY

### Instrumentation and Techniques

The laboratory models were made of 6-in. diameter Perspex cylinders in which a clay layer 18-cm thick was compacted on top of a layer of filter material. A load simulating the overburden pressure on the clay in the field was exerted on the model by a spring setup (Fig. 5). Through holes bored in the Perspex column, tensiometers made of a slender ceramic cylinder and connected to a mercury manometer were in-

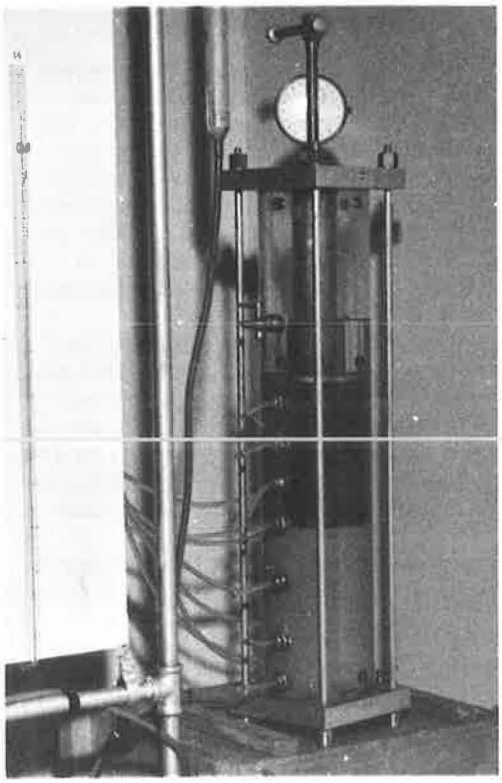

Figure 5. Model of clay layer overlaying sand layer, showing connections to tensiometers and spring setup for load application.

serted into the clay, as well as into the filter material, at various levels including the level of the interface between the two materials. The clay layer was saturated under a head of water and then allowed to swell under the imposed load. Later, any free water in the filter material and on top of the clay was allowed to drain. The clay was then permitted to dry by being exposed to the atmosphere through holes in the plate transmitting the spring load and in the Perspex cylinder. During both cycles of wetting and drying, suction and movement were recorded. The measurements were carried out in a constant temperature room, with a temperature as high as 30 C to accelerate the drying process. The measurements were continued over the period of time required for attaining stable conditions.

The suction measured in the models was converted later into moisture contents by using a moisture-suction curve determined by another apparatus under the same placement and loading conditions (3).

The clay was compacted into the cylinder by a static pressure to a density of 1.40 gm/cu cm at a moisture content of 24 percent. These placement conditions correspond to about 95 percent of the optimum conditions obtained by Modified AASHO compaction. The pressure applied on the layered system in the models was 0.15 kg/sq cm, simulating an overburden of 1 m, corresponding to the depth of the drainage system.

## Experimental Results

Moisture-Suction Relationship of Clay. —The moisture-suction function of the clay during a cycle of drying and wetting is shown in Figure 6. The curve was obtained after saturation of the sample under the same pressure as applied in the models, i. e., 0.15 kg/sq cm.

The apparatus used for suction determination (3) allowed for measurement of suction up to ¾ atmos. However, the range of moisture corresponding to suction up to ¾ atmos. (Fig. 6) is approximately the same as the range of moistures observed in the field (Fig. 4), i.e., 34 to 39 percent, particularly at the depth adjacent to the drainage system.

Suction and Moisture Variations in the Models.

Exposed Clay. —Figure 7 shows the distribution of pressure head with depth in the clay and filter materials during the wetting process achieved by the application of a relatively low head on top of the clay. Figure 7a shows the pressure head distribution for the clay-sand model and 7b for the clay-gravel model. The negative pore pressures (suctions) recorded at the interfaces between the clay and the granular materials are typical for unsaturated flow taking place in clay under low head (4); the suction at the sand interface amounted to about 30 cm of water, whereas the same value for the gravel was about 9 cm of water.

Figures 8a and 9a show the distributions of suction with depth in models measured at different times during the drying process. The clay was allowed to saturate from

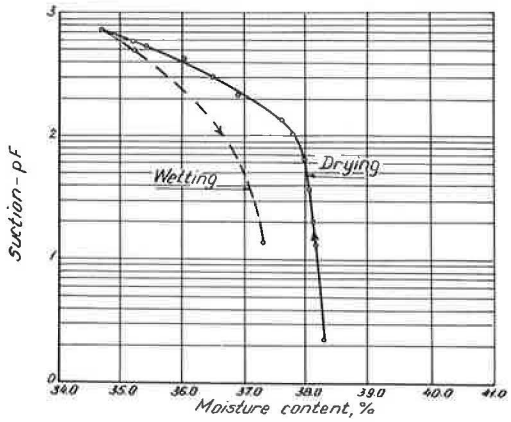


Figure 6. Moisture-suction relationship for clay.

the bottom by application of a relatively high head before drying. The moisture content distributions with depth at the same times, as interpreted from Figure 6, are shown in Figure 8b. The suctions and therefore the moisture changes developed in the clay in contact with the sand were far smaller than in the clay in contact with the crushed stone, after the same period of drying.

Covered Clay. — Figures 10 and 11 show the suction and moisture distributions during the drying process for the models of the covered clay. The moisture content at the interface between the clay and sand has remained virtually unchanged with time. In addition, the variation in moisture through the depth of the clay profile was rather small and amounted to a maximum of 2 percent close to the surface, after 60 days. However, con-

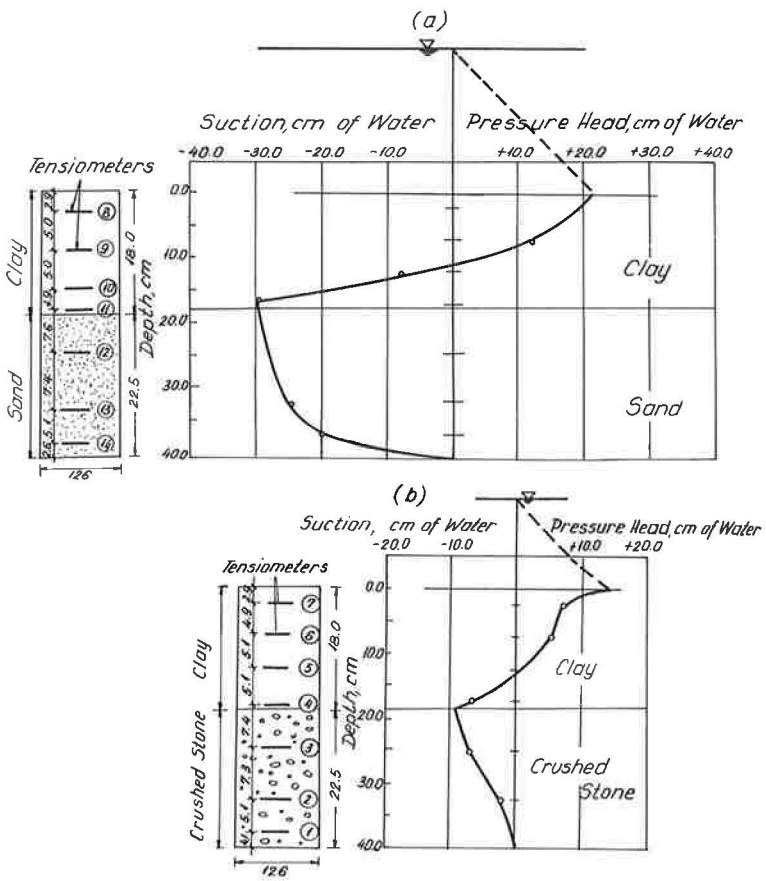


Figure 7. Distribution of pressure-head in uncovered clay models: (a) clay overlying sand, (b) clay overlying crushed stone.

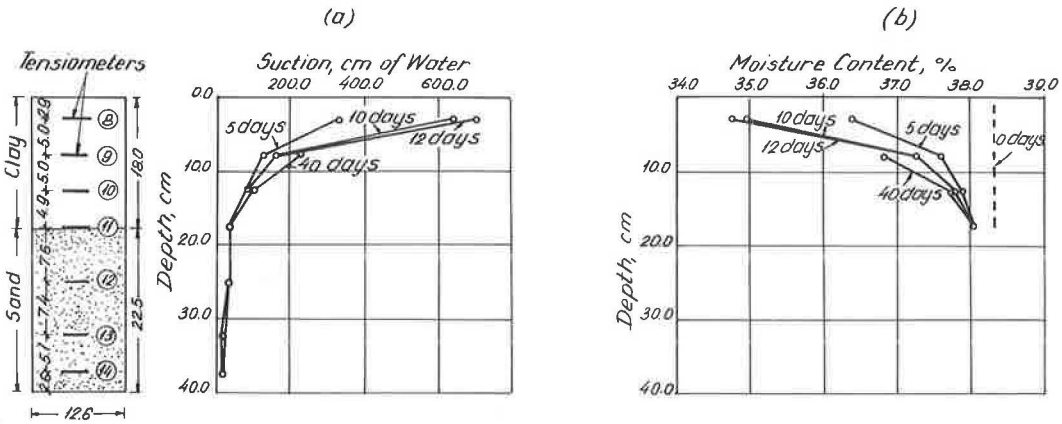


Figure 8. Distribution of suction and moisture with depth on drying of uncovered clay overlying sand.

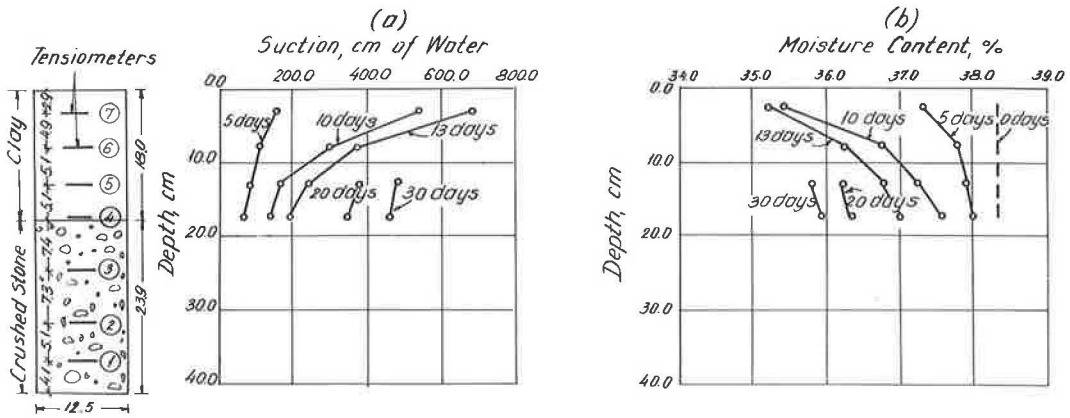


Figure 9. Distribution of suction and moisture with depth on drying of clay overlying crushed stone.

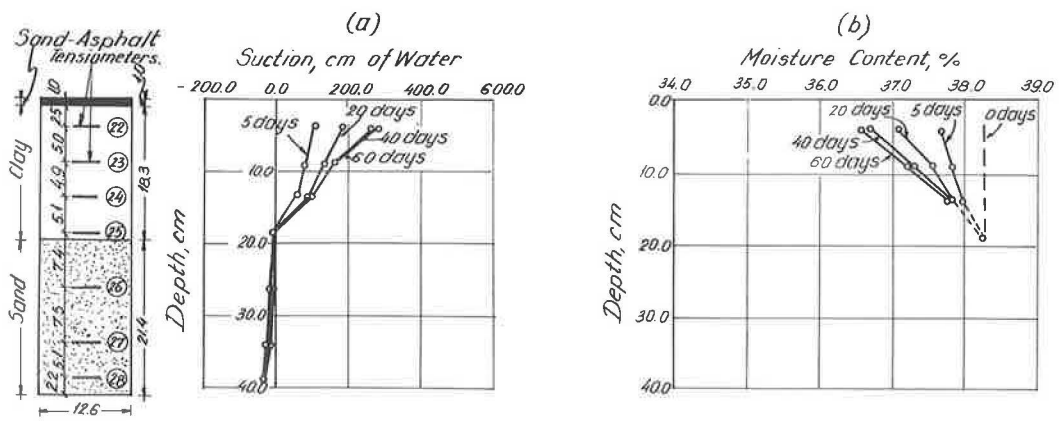


Figure 10. Distribution of suction and moisture with depth on drying of covered clay overlying sand.

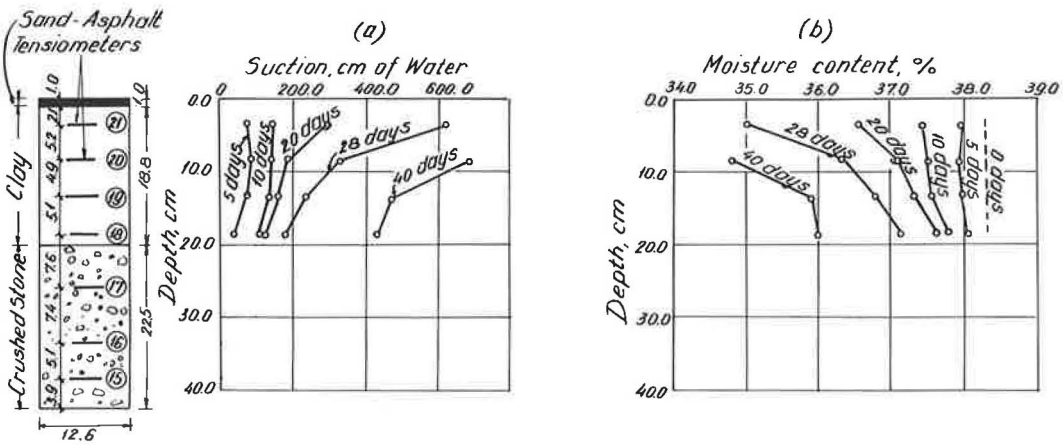


Figure 11. Distribution of suction and moisture with depth on drying of covered clay overlying crushed stone.

siderable suction was recorded at the interface between the clay and the crushed stone, in spite of the cover. Moisture changes throughout the profile in the model were also noticeable and amounted to more than 5 percent after 40 days.

## DISCUSSION

The application of the experimental results from laboratory models is limited from various viewpoints: (a) the thickness of the clay layer in the models was severalfold smaller than the actual thickness of the clay in the field; (b) the clay in the models was remolded and compacted as compared with the natural structure of the clay in the field; (c) usually the clay in the field is located adjacent to the drainage system as compared to the clay overlying the system in the models; (d) moisture in nature moves laterally and vertically, whereas in the models the movement was confined to the vertical direction only; (e) the initial moisture of the clay before the drying process was assumed uniform and corresponds to saturation moisture, as compared to nonuniform distribution in the field; and (f) suction in the field, particularly at the surface, is much higher than was measureable in the models.

Nevertheless, the experimental results may be analyzed mainly from two viewpoints: (a) the significance of the drainage system during the drying state, and (b) the effect of the composition of the filter material on maintaining a stable moisture regime in the clay.

The incorporation of a subdrainage system in highway and runway clay shoulders and selection of the filter material composition are usually determined solely by hydraulic and piping considerations. In semiarid countries, however, where the groundwater table is usually low and the only source of seepage water in the pavement and shoulders originates from percolation, the head of water acting on the subdrainage system is rather low and its duration short. Under such low heads, unsaturated flow takes place (4) resulting in negative pore pressure (suction) at the interface between the clay and the filter materials (Fig. 7). These negative pressures in the pore water increase the effective stress in the clay (5) and decrease the danger of washing out of clay particles or aggregates into the drainage system. From this viewpoint, it would have been possible to select a relatively coarse filter material for the subdrainage system.

The models showed, however, that the composition of the filter material should not be ignored in design because it may play a significant role in establishing a more stable moisture regime in the clay surrounding the drainage system during the drying cycle. Figure 12 shows the moisture changes at the interface between the clay and filter materials under the various cover conditions as a function of drying time. Virtually no moisture changes occurred at the interface between the sand and the covered clay, and

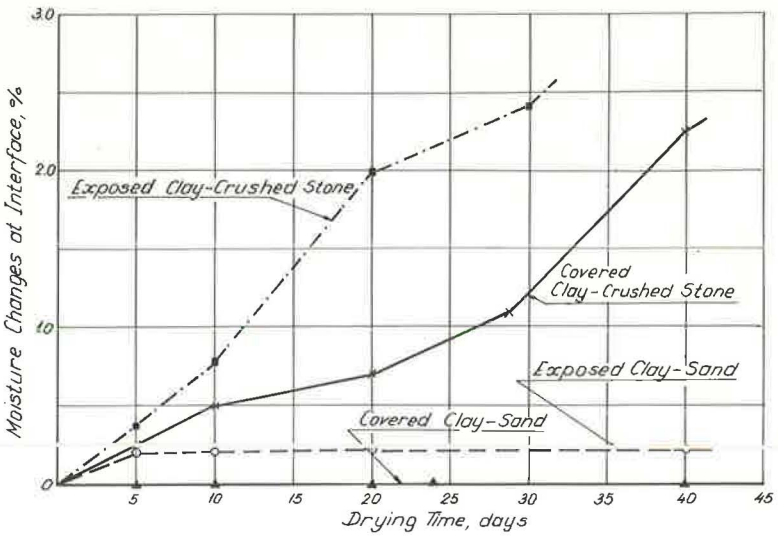


Figure 12. Moisture variations at interface of clay and filter materials under various cover conditions on drying.

very small changes occurred between the same materials under no cover. This means, actually, that the moisture held in the sand tends to serve as a source of moisture for the clay, reducing drying at the vicinity of the subdrainage system. Therefore, under similar conditions in the field, it is desirable that the material selected for the filter be composed of fine sand, to minimize moisture changes on drying.

An approximate calculation of gradients and flux shows that the difference in behavior between the clay overlaying the sand and the crushed stone was due to the removal of water from the sand by the clay. This behavior is responsible for the constant moisture kept within the interface between the sand and clay. Approximately 6 percent of the moisture available in the sand could be withdrawn by the clay while drying. Should drying continue, the sand would tend to act as an effective barrier against drying out of the clay subgrade immediately underneath the pavement edge. For these measures to be effective, however, the trench of the subdrainage system should extend to the depth of seasonal moisture variation and be backfilled with water-holding material, such as fine sand.

## CONCLUSIONS

In spite of the limitations involved in the laboratory model study presented in this paper, the following conclusions may be deduced on the effect of the subdrainage system on the moisture regime in clay shoulders:

1. The subdrainage system has a definite positive effect on the moisture distributions in the clay subgrade. By removing free water which penetrates cracks, the system helps to maintain a low range of moisture variations between summer and winter and thus inhibits large movements at the edge of the pavement.
2. In semiarid countries the selection of the filter material for the drainage system should be governed mainly by criteria of moisture variations in the clay adjacent to the system and not by piping considerations.
3. Under the foregoing conditions, it is desirable to use a fine permeable material for the subdrainage system, since this material would tend to serve both as a moisture reservoir for the clay during the drying period and a barrier against drying out of the clay underneath the pavement.

## ACKNOWLEDGMENTS

Thanks are due to B. Zur for valuable discussions on the drying phenomenon in soils. The model test results were reported by Z. Globinsky (1) and made available to the authors.

## REFERENCES

1. Globinsky, Z. Model Study of Suction, Moisture and Movement Variations in Clay Shoulders of Runways, Technion, Israel Inst. of Tech., M. Sc. thesis, Haifa, Israel, 1964.
2. Wiseman, G. A Study of Expansive Clay Subgrades Under Airfield Pavements. Israel Inst. of Tech., Dr. Sci. thesis, Haifa, 1959.
3. Kassiff, G. and Globinsky, Z. Apparatus for Measurement of Suction Under External Load. Highway Research Record 111, pp. 24-30, 1966.
4. Kisch, M. The Theory of Seepage from Clay Blanketed Resevoirs. Géotechnique, Vol. 9, 1959.
5. Croney, D., Coleman, J. D., and Black, W. P. M. Movement and Distribution of Water in Soil Relation to Highway Design and Performance. Highway Research Board Spec. Rept. 40, pp. 226-252, 1958.

# Model Evaluation of Soil Factors Affecting Rigid Pavement Pumping

WAIN W. STOWE, U. S. Army Corps of Engineers;
RICHARD L. HANDY, Iowa State University; and
JAMES P. FERO, U. S. Army Corps of Engineers

A laboratory model was devised to simulate pumping of an 8-in. nonreinforced rigid pavement under a 9,000-lb wheel load traveling 14 mph. The model pumping action was observed to be a soil erosion phenomenon, and a theoretical approach indicated soil cohesion as a key factor. Tests on several fine-grained soils at different temperatures and different compacted densities verified that pumping rate without drainage is inversely proportional to soil cohesion. Increasing soil density and decreasing soil temperature both retard pumping by increasing cohesion, and stabilizers to inhibit pumping of fine-grained soils may be selected on the basis of their effect on cohesion. Preliminary pumping data on soil-cement are presented.

•PUMPING has been recognized as a major cause of concrete pavement failure since 1945. Although regarded in many states as a minor problem (1, p. 163), pumping was a causal factor in the majority of AASHO Road Test rigid pavement failures (2), and may be expected to increase with increasing truck traffic.

Pumping may be defined as the ejection of soil and water from beneath a rigid pavement, induced by the deflection of the slab at a joint, edge, or crack (Fig. 1a). Heavy axle loads are normally required to deflect the slab sufficiently to promote pumping. Since free water is also required, pumping normally occurs only during or immediately following a rain. The ejection of soil and water forms a void which continues to enlarge until the slab cracks and fails.

During the 1940's exhaustive field surveys were conducted to find the causes of pumping. Results of surveys in Tennessee, North Carolina, Kansas, Illinois, and Indiana (3) concluded that: (a) slow, heavily loaded trucks induce the most pumping; (b) pumping is most severe on uphill grades where truck speed is lowered; (c) pumping soils have over 45 percent combined silt and clay; (d) there is no correlation of pumpability to consolidation and shear strength, although compaction delays pumping; and (e) a granular subbase will prevent pumping.

Since the 1950's many highways have been built on granular subbases, which solved the problem at least temporarily. However, under increasingly severe loading conditions even granular subbases were found to pump or blow, the latter being defined as ejection of granular base materials in an action similar to pumping (1), but usually occurring along slab edges rather than at joints (Fig. 1b). For the present purpose we make no distinction between pumping and blowing, and soil includes granular or treated base or subbase materials immediately beneath the pavement slab.

Paper sponsored by Committee on Strength and Deformation Characteristics of Pavement Sections.



Figure 1. (a) Pavement pumping; ejection of mud and water; (b) blowing; ejection of sand and water.

## LABORATORY MODELS

A model approach allows isolation and evaluation of pertinent variables at the expense of introducing uncertainties regarding the relationship between the model and the field prototype situation. In 1957 a model was built by the Portland Cement Association (4) to about one-half scale; it had a 2-in. thick concrete slab, and required 2 cu yd of base material. The slabs were loaded simultaneously, an action not occurring under actual pavements.

Principal findings from the PCA study were that better compaction reduces granular subbase pumping. Pumping was observed in subbase material containing more than 10 percent passing the No. 200 sieve. Use of a subbase reduced pumping, and a granular soil-cement did not pump.

Another model was devised about the same time by Havers and Yoder (5), using an 8- by 6-in. vertically oriented cylindrical sample agitated by a piston from above. The pumping action was recognized as involving not only an erosion by the ejection of water, but also a migration and selective removal of fines from a base course, and an upward intrusion of subgrade material into a base course. Again, the loading did not duplicate the one-two slap action of slabs at pavement joints. Their results indicated that (a) a highly plastic residual clay from weathering of limestone (Frederick series) pumped less than a moderately plastic silty clay glacial soil (Crosby series); (b) increased compaction decreased deflections; (c) increased pavement pressure increased pumping; and (d) an open-graded base pumps less than one containing generous amounts of fines. A further study by Chamberlin and Yoder (6) indicated that the critical contents of minus 200 sieve material to cause pumping are over 3 percent for a gravel base or over 12 percent for a sand base.

These model studies of pumping emphasized gradation effects, and filter design theory was suggested to prevent selective grain movements or intrusions.

A smaller model was designed by Reign in 1961 (7). He utilized a 2- by 2-in. cylindrical soil sample with the load applied in a sinusoidal fashion from two semicircular plates which remained in contact with the soil. Reign found a correlation to group index; the higher the index over 4, the more the pumping. Although the model represented the alternating loading condition at a joint, it did not simulate the sudden slap received by the soil under the departure slab as the load crosses the joint. Also, the edge effects from the small sample and calibration problems made correlation of data difficult.

Another model, devised by the authors in 1963, is used in this study. The objectives were to devise a realistic model and attempt to evaluate the effects of various factors such as temperature, soil type, density, texture, shearing strength, and effects of stabilizers.

## DESCRIPTION OF APPARATUS

The essential elements of the model are shown in Figure 2a. A 31-in. diameter drive wheel with eight 3-in. diameter rubber rollers to transmit the load is mounted

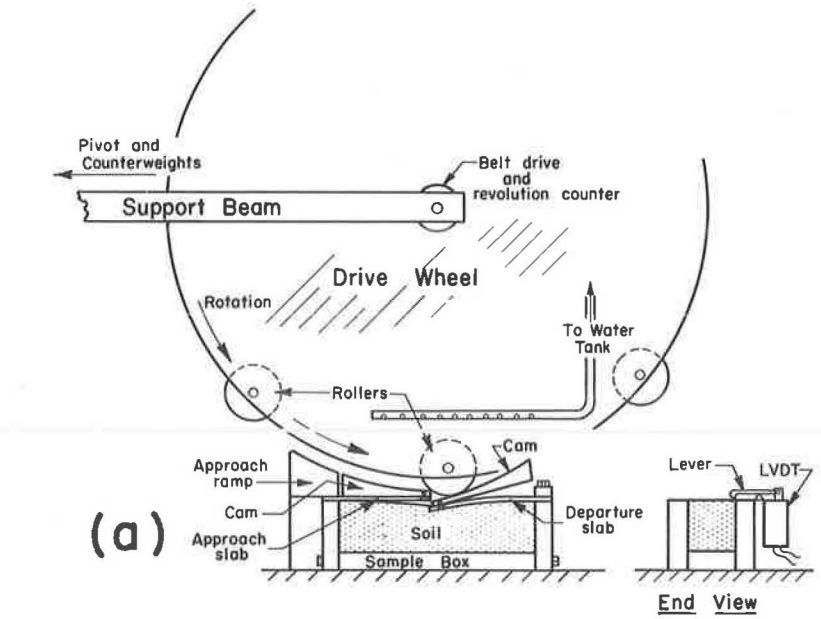


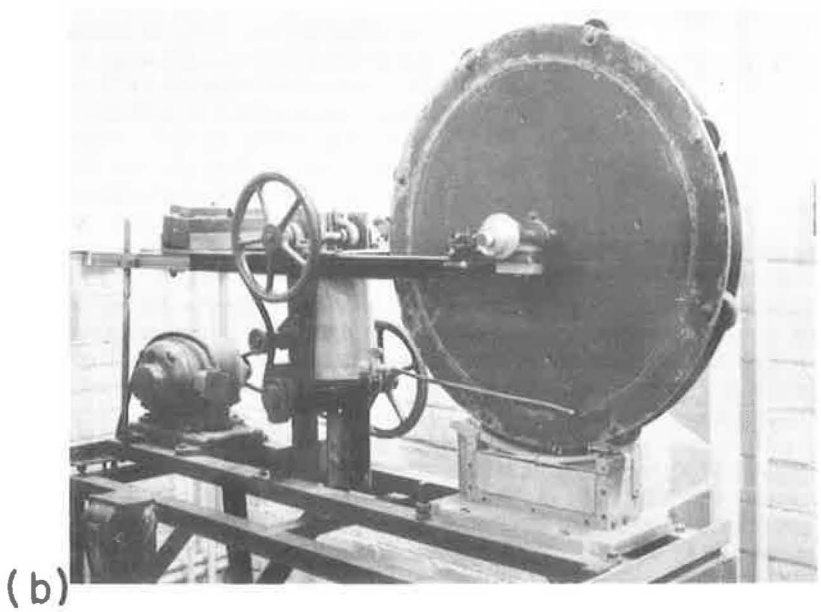


Figure 2. (a) Schematic of pumping apparatus. Soil sample is 3 by 3 by 11 ¼ in.; rollers are 3-in. diameter and move at 3 mph. (b) Overall view of the pumping apparatus with plexiglass sample box front removed to show soil-cement sample after pumping.

at the end of a 5-ft beam, 2 ft from a pivot. An adjustable weight is attached to the beam beyond the pivot as a counterbalance, and an electric motor turns the drive wheel at an angular velocity of 30 rpm. A sample box to hold standard 3- by 3- by 11 ¼-in. compacted flexural test specimens (ASTM Designation D 1632-63 (8)) is cen-

tered under the axis of the drive wheel. The simulated pavement slabs are $\frac{1}{16}$-ft sheet titanium, chosen for its high resistance to fatigue.

One problem was to translate the arc path of the rollers to the horizontal plane of the slabs; this was done with aluminum cams concave to the path of the rollers (16 $\frac{1}{2}$-in. radius) and attached near the slab joint to allow uniform bending of the slabs as the load crosses.

A second problem was how to avoid impact loading of the approach slab. This was done with an aluminum ramp bolted to the sample box; as one roller leaves the departure slab, the weight of the drive wheel is transferred to the next roller on this approach ramp.

Deflections are measured at two locations on each slab, at the middles and at the joints. Vertical displacements of the slabs are transmitted by levers (Fig. 2a) to cores inside four linear variable differential transformers (LVDT's). The LVDT's convert the linear deflections into discrete a.c. voltage changes which are sent to rectifiers, amplifiers, and a four-channel rapid scan recorder. A microswitch on the large wheel actuates an event counter on the recorder every eight repetitions of loading. Thus the amounts of deflection vs number of repetitions are continuously plotted on the recorder chart.

## MODEL ANALYSIS

The machine was originally conceived to be analogous to an 18,000-lb axle load traveling at various speeds. A preliminary analysis was performed by considering relative tire print sizes and their contact times. Prints from the model tires average 0.375 sq in., so for a contact pressure of 75 psi the roller load must be 28 lb. As a check, the load giving a maximum slab contact pressure of 7 psi, to correspond to the PCA experiments (3), was calculated, taking 100 pci as the modulus of subgrade reaction. Calculated this way, the model tire load is 26.5 lb.

The model tire print length is 0.50 in., compared to about 10 in. measured on a loaded truck, which means that for the same tire contact time at any point as a truck traveling at 60 mph, the model wheel should travel 3 mph.

The 28 lb and 3 mph were used for design. A more sophisticated model analysis revealed some inconsistencies and velocity distortions, a distorted model being inevitable because it is impossible to scale down all the various soil and fluid factors.

A partial list of variables might include:

$n^*$, number of repetitions;
W, wheel load, M;
V, wheel velocity, $LT^{-1}$;
A, wheel contact area, $L^2$;
L, acting slab length, L;
P, acting slab perimeter, L;
$d^*$, deflection, L;
$s^*$, any soil grain size, L;
$\rho^*$, density of fluid, $ML^{-3}$;
$\mu^*$ viscosity of fluid, $ML^{-1}T^{-1}$;
$\sigma^*$, surface tension of fluid, $MT^{-2}$;
E, slab modulus of elasticity, $ML^{-2}$;
I, slab moment of inertia, $L^{-2}$; and
$g^*$, acceleration of gravity, $LT^{-2}$.

Variables not scaled in the model are starred. (Others whould include soil specific gravity, cohesion, density, and moisture content.) From these variables, a series of dimensionless $\pi$ terms may be written:

$$n = f\left(\frac{d}{s}, \frac{W}{A\rho s}, \frac{V^2}{gP}, \frac{\rho V^2 P}{\sigma}, \frac{\rho V P}{\mu}, \frac{L}{P}, \frac{L^2}{A}, \frac{L}{s}, \frac{WL^2}{EI}, \frac{AE}{W}\right) \quad (1)$$

According to principles of similitude, corresponding $\pi$ terms should be equal in the model and in the prototype field situation (9). If this is true or if the distortions are

of no consequence, n, the number of repetitions, should be equivalent in model and prototype.

The condition of equality of the second $\pi$ term is readily satisfied, i.e., since s is the same in the model as in the prototype, d should be the same also; if a deflection of 0.10 in. is taken as incipient failure in the pavement, 0.10 in. is the analogous deflection in the model. The third term dictates that W/A should be the same in model and prototype; both are nominally 75 psi. The fourth, fifth, and sixth terms cannot be simultaneously satisfied. They are dimensionally analogous to the Froude, Weber and Reynolds numbers, representing inertial, surface tension, and viscous effects, respectively. For reasons discussed later relating erosion to impulse and momentum, the Froude number appears most pertinent, and the other two terms were ignored. According to the fourth $\pi$ term, if the field pumping perimeter P is 25 ft, the truck speed corresponding to a model speed Vm of 3 mph is only about 14 mph. The velocity variable was to have been investigated, but could not be because of lack of affluent sponsors. As previously mentioned, field data indicate more pumping at low than at high vehicular speeds (3).

The seventh $\pi$ term, L/P, for the model is 0.394, so for a field active or pumping perimeter of 25 ft, the length of cantilever slab L should be about 10 ft. In the absence of actual measurements all that can be said is that this appears to be the correct order of magnitude. The analogous dimension for edge pumping would be some diagonal vector representing the direction of water movement, about which even less is known. The eighth term suggests a constant ratio between L and tire print length; scale factors for both are about 20. The ninth term, L/s, is necessarily distorted and we assume it is not important. The tenth term which describes bending in flexure is approximately satisfied, the $\frac{1}{16}$-in. titanium model slab corresponding to about 8 in. of nonreinforced concrete. The last term is indicative of slab warping under the respective wheel loads and indicates warping will be less in the model.

To summarize, the pumping machine is a distorted model with horizontal linear dimension scale factors of about 20, and vertical deflection, soil and fluid property, and unit load scale factors of one. Contrary to original plan, the model was only operated at one speed, corresponding to a truck speed of about 14 mph.

## EROSION

Model trials indicated that pumping is essentially an erosion phenomenon, material under the model slabs being eroded and removed with the ejecting water. Erodibility of sediments at various water velocities was plotted by Hjulstrom (10), who found that fine sands are most readily eroded, both coarser and finer sizes being more resistant. Resistance of clay was attributed to cohesion.

An influence from clay mineralogy is suggested by a soil erosion study by Lutz (11), who found that calcium saturation decreased erodibility of a montmorillonitic soil (Iredell series), and that a kaolinitic clay soil (Davidson series) was even less erodible. Lutz' results may have been strongly influenced by permeability and infiltration rates. Erosion by artificial raindrops also increases with increasing sand and decreases with aggregation (12, p. 38). André and Anderson suggest that erodibility depends on the ratio of binder (clay) to readily erodible particles (sand) (13).

Horton (14) applied principles of fluid mechanics to the open flow erosion process, theorizing that erosion will take place when the force provided by the flow of water exceeds the shearing resistance of the soil. Horton's equation, derived on the basis of energy considerations, relates erosive force to slope and depth of flow.

Another approach is a fluid mechanics consideration of impulse and momentum, which shows that drag on a body by a fluid of density $\rho$ and constant velocity, $V_f$, relative to the body is

$$D = k_D \rho a_y V_f^2 \qquad (2)$$

where

D = drag,

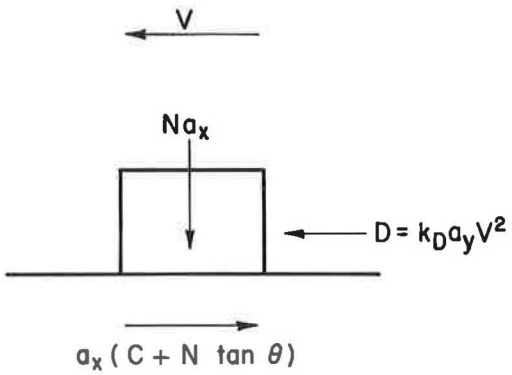


Figure 3. Erosive and resistant forces on a soil grain.

$k_D$ = a drag coefficient, and

$a_y$ = the area of the object normal to the direction of flow.

Opposing D is shear (Fig. 3), or for incipient erosion,

$$D \geq a_x g(c + N \tan \theta) \qquad (3)$$

where

$a_x$ = grain base contact area,
g = acceleration of gravity,
c = unit cohesive shear strength of contact,
N = normal stress from immersed weight of soil grain, and
tan θ = coefficient of sliding friction at contact[a].

For a cubic grain,

$$a_x = d^2, \text{ and} \qquad (4)$$

$$N = d(\rho_s - \rho) \qquad (5)$$

where $\rho_s$ is the density of the grain. Substituting and combining equations,

$$D = k_d \rho \; V_f^2 \; d^2 \geq g d^2 \left[ c + d(\rho_s - \rho) \tan \theta \right] \qquad (6)$$

$$V_f^2 \geq \frac{g}{k_d \rho} \left[ c + d(\rho_s - \rho) \tan \theta \right]$$

or

$$V_f^2 \geq C \left[ c + d(\rho_s - \rho) \tan \theta \right] \qquad (7)$$

where C may be called a coefficient of erosion, and will vary somewhat depending on grain shape and alignment. (Dimensions of C are $L^4 T^{-2} M^{-1}$)[b].

Therefore, if unit cohesion c = 0, as for sand or gravel, the erosion velocity, V, should be proportional to the square root of the grain diameter.

Or if the grain size, d, or the coefficient of friction are very small, as for a clay, erosion velocity, V, should be proportional to square root of the cohesion (more correctly the cohesive shear strength).

The relationship between V and erosion rate will be through some unknown probability function. That is, fluid velocities in turbulent flow have an exceedingly random distribution about an average; raising V, the threshold for erosion, should reduce the probability of encountering a fluid velocity sufficient to erode, and hence reduce the rate of erosion.

---

[a] Tan θ was used rather than tan φ to distinguish sliding friction from internal friction, which is influenced by bulking during shear.

[b] A similar approach by Leopold, Wolman and Miller (12, p. 172) assumes that the force to move the particle must overcome the weight of the particle; presumably the initial movement would be by tipping rather than sliding, as assumed previously. Making no allowance for cohesion, they also concluded that V for erosion is proportional to $\sqrt{d}$, and point out that in open channel flow $V_f \simeq \sqrt{\tau}$, where τ is the resistance to flow, and therefore $d \simeq \tau$. This they illustrate with experimental data. In another derivation after Leopold (12, p. 175) frictional resistance is considered, but again cohesion is not taken into account.

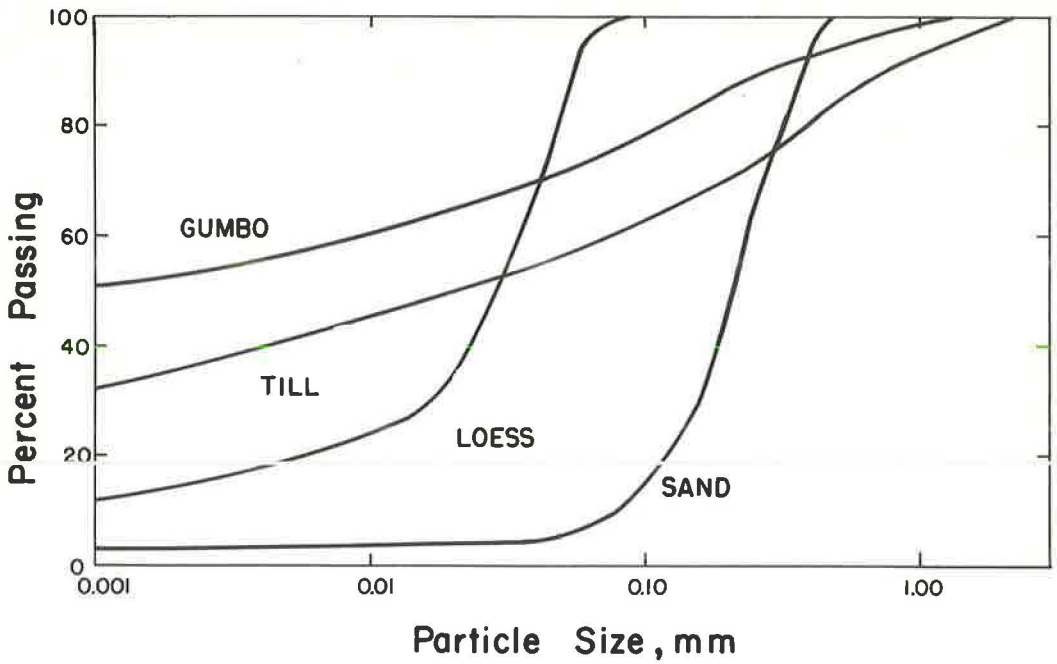


Figure 4. Particle-size accumulation curves of four soils tested for pumping.

Another factor influencing erosion rate is that of protective cover, the most erodible grains will be selectively removed, leaving a lag concentrate or particles with a lower probability of erosion. This is analogous to the desert pavement of wind-swept arid areas. Still another factor is sand-blasting by suspended particles, wherein momentum (mass times velocity) tends to be preserved or transferred to other particles on impact.

## TESTS

Four relatively fine-grained soils were selected for test: an aeolian fine sand, a loessial silt, a glacial till loam, and a fossil B-horizon gumbotil clay. Grain size curves are presented in Figure 4; properties are given in Table 1.

The soil samples were molded to either standard or modified Proctor density according to ASTM Designation D 1632-63 (8) for 3- by 3- by 11 ¼-in. flexural test specimens were usually wrapped and allowed to cure at 100 percent humidity 2 days to equilibrate moisture within the sample, release residual stresses, and allow development of thixotropic effect. Most samples swelled during curing and were trimmed back with the aid of a trimming box.

### Pumping Action

As the soils pumped, a rigorous erosion action was readily observable through the Plexiglass box front. During the tests, muddy water was squirted about to the extent that splatter shields were added to the apparatus. Typical experimental results are shown in Figure 5. In most instances the slab deflection was proportional to n, the number of repetitions.

Most samples eroded more rapidly under the departure slab, probably because the sudden impact loading of this slab visibly increased fluid ejection velocity. The result was a step analogous to joint faulting in the field (Fig. 6a). Another field condition observed in the model was a tendency to accumulate loose sand back under the slab, which would tend to tilt the slab and accentuate joint faulting if there were no end re-

TABLE 1

PROPERTIES OF SOILS STUDIED

| Characteristic | Soil | | | |
|---|---|---|---|---|
| | Dune Sand | Friable Loess | Kansan Glacial Till | Gumbotil |
| Lab No. | S-6-2 | 20-2 | 409-C | 528-8 |
| Classif. | | | | |
| AASHO/ASTM | A-3(0) | A-4(8) | A-7-6(14) | A-7-6(20) |
| BPR | Sand | Silt loam | Clay | Clay |
| USDA | Sand | Silt | Clay | Clay |
| County in Iowa | Benton | Harrison | Ringold | Keokuk |
| Soil series | Carrington | Hamburg | Shelby | Muhaska |
| Horizon | B | B | B | B |
| L. L. (%) | - | 32 | 50 | 65 |
| P. L. (%) | - | 27 | 17 | 24 |
| P. I. | N. P. | 5 | 33 | 41 |
| Dom. clay mineral[a] | Mont. | Mont. | Mont. | Mont. |
| Dom. exch. cation[a] | $Ca^{++}$ | $Ca^{++}$ | $Ca^{++}$ | $Ca^{++}$ |

[a]From X-ray diffraction and DTA.

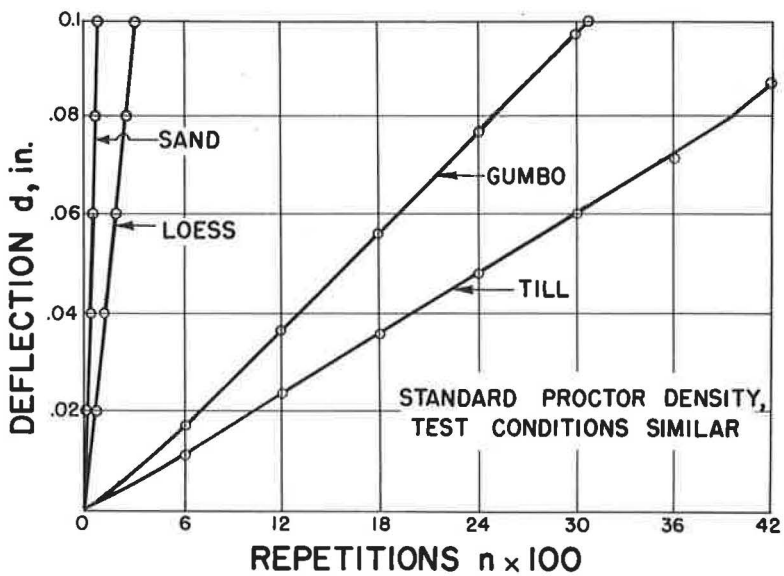


Figure 5. Representative pumping test results.

straints. Clayey samples removed from the machine often showed an interesting pattern of erosion channels between sand-capped mesas (Fig. 6b). Pumping stopped immediately if the water supply was shut off.

## Pumping Resistance

Drainage was prevented by the sample box, and the silt and fine sand pumped very rapidly to the arbitrary failure deflection of 0.1 in. (Table 2). The till and gumbotil pumped much more slowly, glacial till being the slowest. Compaction to

TABLE 2

PUMPING TEST RESULTS[a]

| Characteristic | Soil | | | | | | | | | | | |
|---|---|---|---|---|---|---|---|---|---|---|---|---|
| | Dune Sand | | | Loess | | | Glacial Till | | | Gumbotil | | |
| | Std. | Comp. | Mod. Comp. | Std. | Comp. | Mod. Comp. | Std. | Comp. | Mod. Comp. | Std. | Comp. | Mod. Comp. |
| Opt. Moist. Cont. (%) | 9.5 | | 8.6 | 15.2 | | 15.0 | 15.0 | | 12.3 | 23.2 | | 17.5 |
| Density, pcf | 112 | | 118 | 110 | | 118 | 116 | | 125 | 96 | | 109 |
| Direct shear: | | | | | | | | | | | | |
| c (psi) | 1.6 | | - | 10 | | - | 63 | | 73 | 40 | | 66 |
| $\phi$ (deg) | 33.9 | | - | 34.0 | | - | 13.8 | | 47.5 | 8.3 | | 35.0 |
| n for 0.1-in. defl. | 47 | | 103 | 476 | | 500 | 5,194 | | 5,520 | 3,049 | | 5,403 |

[a]All maximum deflections occurred at the joint and on the departure slab.




Figure 6. Tested specimens: (a) top view of gumbo, showing sand-capped mesas, 2,600 repetitions; (b) oblique view of soil-cement showing step, 20,000 repetitions.

modified Proctor density increased pumping resistance, as indicated in Table 2.

## Strength Tests

For comparison purposes, direct shear tests were performed on the soil samples, giving c and $\phi$ values reported in Table 2. The angle of internal friction apparently has little influence on pumping, but cohesion appears closely related to pumping resistance. A graph of n vs c is shown in Figure 7, and gives a linear relationship with a correlation coefficient r = 0.994, a value of 1.0 indicating perfect correlation. Other relationships of n to percent clay, to P. I., to P. I./percent clay, to median grain size, to sorting coefficient, etc., were much less consistent.

## Temperature

Tests were made on the silt at different temperatures from 3 to 50 C to find the influence of viscosity and/or changing cohesion. Results are given in Table 3; it will be noted that higher temperatures gave faster pumping.

To determine whether the influence of temperature was one of changing fluid viscosity or changing cohesion, direct shear tests were performed. These gave for the silt:

$$c = 12.5 - \frac{T}{8}$$

where T is degrees centigrade and c is

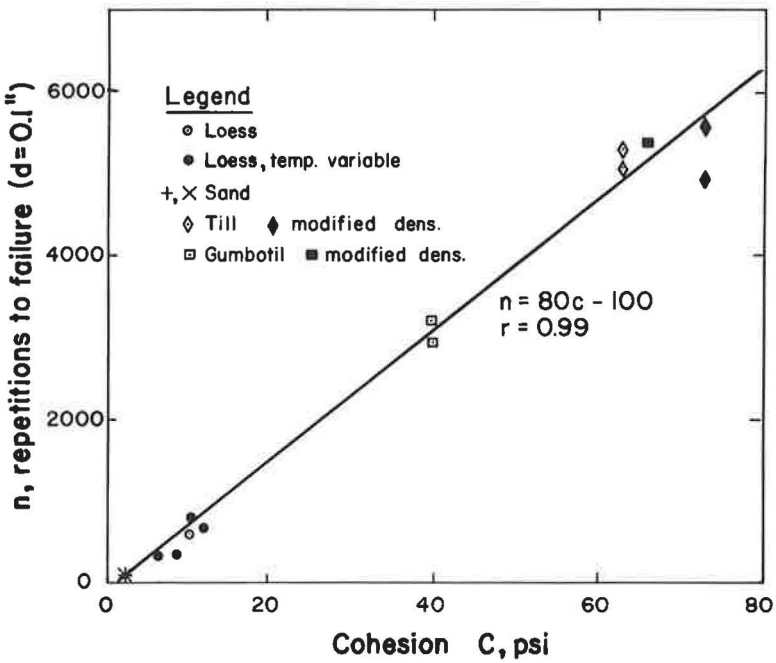


Figure 7. Relation between repetitions to failure and soil cohesion by direct shear test.

TABLE 3

EFFECTS OF TEMPERATURE AND STABILIZERS

| Soil | Temperature, °C | | Additives | Curing | n for 0.1-in. Defl. |
|---|---|---|---|---|---|
| | Soil | Water | | | |
| Loess, | 3 | 3 | - | - | 685 |
| Std. | 15.5 | 15.5 | - | - | 750 |
| Dens. | 21 | 21 | - | - | 630 |
| | 33 | 33 | - | - | 316 |
| | 50.5 | 50.5 | - | - | 320 |
| Till, mod. | 23 | 22 | - | - | 5,600 |
| Dens. | 5 | 22 | - | - | 6,000 |
| Loess | 26 | 26 | - | - | 335 |
| | 26 | 26 | 0.2% Arq. 2HT | - | 340 |
| | 26 | 26 | 0.2% Arq. 2HT | 2 day air dry | 310 |
| 75% sand + 25% loess | - | - | 6% cement | 7 day m.c. | 5,500[a] |

[a]Data approximate.

cohesion in psi. Points of n vs c corrected for temperature are shown as solid dots in Figure 7 and were included in the correlation analysis. The influence of temperature, therefore, appears to be largely in its effect on soil cohesion.

In one test of glacial till the soil was initially 22 C and the water was 5 C. If viscosity of the water were the controlling factor, retardation of pumping should have been immediate. Instead, no effect was noticed until after about 1,600 repetitions, or 15 min., when the soil apparently cooled sufficiently to retard pumping.

### Soaking Effect

The gumbotil clay specimen compacted to modified density was allowed to soak in water 12 hr before testing. There was little or no apparent effect, as is shown in the correlation analysis of Figure 7. Two other tests on the gumbotil at modified density gave higher n's, but were eliminated because of sticking down of the departure slab.

### Soil Stabilizers

The results indicate that pumping of fine-grained soils should be controllable by altering their cohesion. To test this premise two stabilizers were tried, a waterproofer and a cementing agent.

An organic cationic water proofer (Armour Co. Arquad 2HT) was selected for the test because it has very little effect on cohesion and when used in optimum amount it imparts water-repellent properties to the soil (15). Results indicated that 0.2 percent cationic waterproofer with and without air curing did not alter pumpability of the loess.

Incorporation of 6 percent cement in a sandy silt base course mix gave n = 5,500, several hundred times more than unstabilized sand. Cohesion of this mix was not measured, but is probably in the range of 20 to 80 psi (16). According to Fig. 7, c should be about 70 psi.)

Further testing was terminated because of lack of research support.

## CONCLUSIONS

1. In a model devised to simulate rigid pavement pumping, pumping was observed to be mainly a process of erosion by ejection, which can be stopped by shutting off the water.
2. In an undrained situation or where rainfall exceeds rate of drainage, there is an excellent inverse linear relationship between rate of pumping and soil cohesion as measured by the direct shear test.
3. Modified Proctor compaction reduces pumping by increasing cohesion.
4. Lower soil temperature means slower pumping because of improved cohesion.
5. Cement increases pumping resistance of soils, whereas use of a noncohesive waterproofer does not.
6. Because of the relationships to cohesion, unconfined compressive strength should be an approximate measure of pumping resistance of treated and untreated fine-grained soils.

## REFERENCES

1. Yoder, E. J. Principles of Pavement Design. New York, John Wiley and Sons.
2. The AASHO Road Test, Rept. 5, Pavement Research. Highway Research Board Spec. Rept. 61E, 1962.
3. Allen, Harold. Final Report of Project Committee No. 1, Maintenance of Concrete Pavement as Related to the Pumping Action of Slabs. Highway Research Board Proc., Vol. 28, pp. 281-310, 1948.
4. Colley, B. E., and Nowlen, J. W. Performance of Subbases for Concrete Pavements Under Repetitive Loading. Highway Research Board Bull. 202, pp. 32-58, 1958.
5. Havers, J. A., and Yoder, E. J. A Study of Interactions of Selected Combinations of Subgrade and Base Course Subjected to Repeated Loading. Highway Research Board Proc., Vol. 36, pp. 443-478, 1957.

6. Chamberlin, W. P., and Yoder, E. J. Effect of Base Course Gradation on Results of Laboratory Pumping Tests. Highway Research Board Bull. 202, pp. 59-79, 1958.
7. Reign, L. L. Development of an Apparatus and Procedure for Evaluating the Pumping Characteristics of Soil. Iowa State Univ. of Sci. and Tech. Unpubl. M. S. thesis, Ames, Iowa, 1961.
8. 1964 Book of ASTM Standards, Part 11, Amer. Soc. for Testing and Materials, Philadelphia, 1964.
9. Murphy, Glenn. Similitude in Engineering. New York, Ronald Press Co., 1950.
10. Hjulstrom, Filip. Transportation of Detritus by Moving Water. In Trask, Parker D., Recent Marine Sediments, pp. 5-31. Am. Assoc. Pet. Geol. Tulsa, Okla., 1939.
11. Lutz, J. F. The Relation of Soil Erosion to Certain Inherent Soil Properties. Soil Sci. Vol. 40, pp. 439-457, 1935.
12. Leopold, L. B., Wolman, M. G., and Miller, J. P. Fluvial Processes in Geomorphology. San Francisco, W. H. Freeman and Co., 1964.
13. André, J. E., and Anderson, H. W. Variation of Soil Erodibility with Geology, Geographic Zone, Elevation, and Vegetation Type in Northern California Wildlands. Jour. Geophys. Res., Vol. 66, pp. 3351-3358, 1961.
14. Horton, R. E. Erosional Development of Streams and Their Drainage Basins: Hydrophysical Approach to Quantitative Geomorphology. Geol. Soc. Amer. Bull. 54, pp. 275-370, 1945.
15. Hoover, J. M., Davidson, D. T., and Roegiers, J. V. Miniature Triaxial Shear Testing of a Quaternary Ammonium Chloride Stabilized Loess. Iowa Acad. Sci. Proc. 65, pp. 323-331, 1958.
16. Laguros, J. G., and Davidson, D. T. Effect of Chemicals on Soil-Cement Stabilization. Highway Research Record 36, pp. 173-208, 1963.
17. Taylor, Michael A., and Broms, Bergt B. Shear Bond Strength Between Coarse Aggregate and Cement Paste or Mortar. ACI Jour., Proc., Vol. 61, No. 8, pp. 939-957, Aug. 1964.

# Apparatus for Measuring Suction Under External Loads

G. KASSIFF and Z. GLOBINSKY
Respectively, Senior Lecturer and former Research Student, Faculty of Civil Engineering, Israel Institute of Technology

An apparatus which measures negative pore pressures during drying and wetting processes under external loads is described, and test results on a heavy clay and a sand are presented. The present apparatus continuously measures suctions under external loads (negative pore pressures) in a single operation and determines moisture contents without removing the soil sample from the suction plate, thus avoiding interference in the contact between the soil and the plate. For the range of measurable suction the apparatus produced a compressibility factor, $\alpha$, equal to unity for the heavy clay and equal to approximately zero for the sand, which agrees with the British Road Research Laboratory (RRL) work.

•THE ENGINEER RESPONSIBLE for the design of pavement foundations is primarily concerned with the soil above the water table, in which the pore pressures are negative. These pressures are functions of the moisture regime in the soil and of the applied loads. Prediction of changes in the moisture content distribution occurring when the soil is covered and loaded is of great interest in highway and airfield construction.

During the last decade, the British Road Research Laboratory (RRL) made a major contribution to this field (1, 2, 3, 5) by developing theories, instrumentation, and techniques, coupled with field experiments, for the evaluation of moisture changes occurring in the subgrade under various types of cover. From these changes other soil characteristics, such as strength and volume change, were predicted. This work was summarized by Croney and Coleman (3) and discussed by Penner (4).

It is well established now that the surface forces by which water is retained in the soil structure cause pressure reduction (below atmospheric) known as the soil moisture suction, or tension. This term has been reserved by the RRL for pressure reduction in a small sample of the soil, measured when the soil is entirely free from externally applied stresses. A relatively simple apparatus is used for the detection and measurement of soil suction, in which the suction of the soil moisture is balanced by a suction applied to the system.

In the ground, however, the soil is subjected to stress by the surrounding soil as well as by external loads. Since the stress may be effective in changing the stress-free suction of the moisture in a soil element, the pressure of the water in the soil pores, generally known as the pore water pressure, can be regarded as the algebraic sum of two components, i. e., the suction and the effect on the suction of the applied stress, as follows (1, 2, 3, 5):

$$u = s + \alpha p \qquad (1)$$

in which

u = pore pressure when sample is loaded (negative),
s = suction pressure with no loading (negative),

Paper sponsored by Committee on Physico-Chemical Phenomena in Soils.

p = applied pressure (positive), and
$\alpha$ = change of negative pore pressure at constant moisture content, termed compressibility factor.

The compressibility factor, $\alpha$, can be measured directly by a series of loading tests on a sample of known suction. The technique used by RRL (3) consists of inclosing the sample in a thin membrane and subjecting it to increments of all-round pressures. The effect of each increment of external pressure on the pore pressure is measured by adjusting the suction applied to the system to give a static condition of the measuring meniscus in a flow tube connected to the soil sample.

The value of $\alpha$ may vary between unity and zero, depending on the degree of saturation and type of soil. Heavy clays remain saturated down to a moisture content corresponding to the shrinkage limit, and, therefore, $\alpha$ is equal to unity for these soils. Partly saturated sands exhibit a value of $\alpha$ close to zero. Other typical values (2) ranged from $\alpha = 0.15$ for sandy clays to $\alpha = 0.5$ for silty clays.

The RRL method of determining the negative pore pressure, u, has the main disadvantage of carrying out the measurements by two different apparati using two different samples, one for the suction and the other for $\alpha$. Also, the compressibility factor, $\alpha$, is measured by applying a uniform all-round pressure, whereas the soil element in nature is subjected to different pressures in the vertical and horizontal directions. It would, therefore, be desirable to develop an apparatus which would continuously measure the negative pore pressure under drying conditions in a single operation and subject the soil sample to different stresses in the vertical and horizontal directions.

This paper reports progress of work on development of a tensiometer for determination of moisture-suction under load (negative pore pressure) function, which conforms with the requirements specified previously. The range of measureable suction

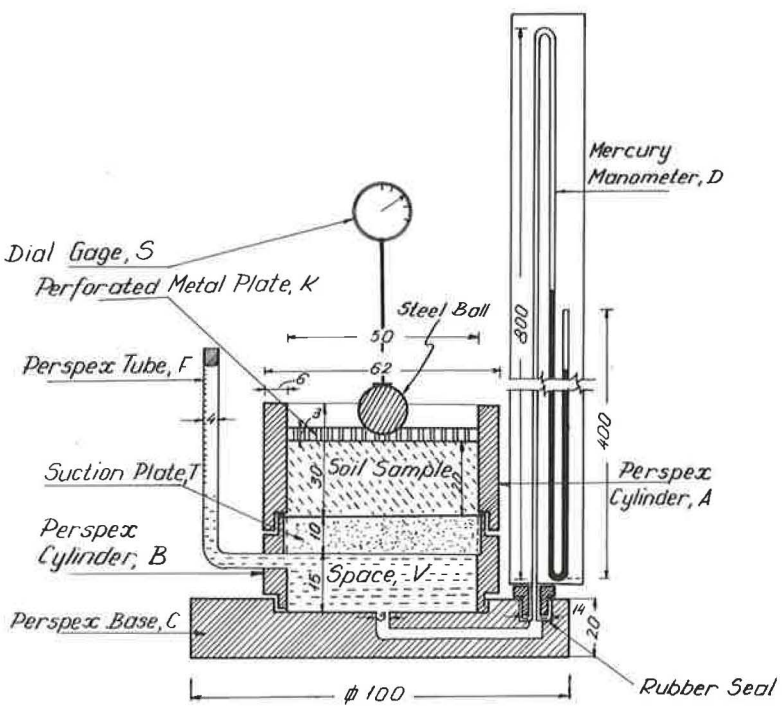


Figure 1. Detailed section of tensiometer.

at this stage, however, is limited to ¾ atmos. Continuation of the work to increase the range of measureable suctions, as well as the number of soils tested, is underway (6).

## DESCRIPTION OF APPARATUS

The apparatus consists of a tensiometer made of a suction plate and a manometer mounted on a loading frame.

Figures 1 and 2 show a detailed drawing and a closeup photo of the tensiometer. The latter consists of a Perspex cylinder, 50-mm I. D., made of two parts, A and B, screwed to a Perspex base, C. At the top of part B a suction plate, T, is fitted, below which the space, V, was filled with deaired distilled water. The soil sample, 30 mm high, is placed on top of the suction plate. The sample is covered with a light metal plate, K, and a steel ball to allow for uniform distribution of the external load on the sample. The plate, K, is perforated for the purpose of wetting as well as drying to the air of the sample. A dial gage, S, is mounted on the ball to measure movement of the soil on swelling and shrinkage. The suction plate, T, is connected through the space, V, to a graduated stand-tube, F, for the purpose of measuring accumulation of air entrapped during the saturation process. A mercury manometer, D, is connected through the base to the suction plate, T.

The tensiometer is placed on a loading frame, which allows for the application of load to the soil sample through a lever system. Figure 3 shows the loading setup.

## TEST PROCEDURE

After saturating the suction plate by applying vacuum through the base C, the soil sample is compacted by a static pressure into the Perspex cylinder A. The two parts of the cylinder, A and B, are then fitted tightly to each other to secure close contact between the soil sample and the suction plate. The apparatus is placed on the loading frame and the desired pressure applied on the soil sample. Under this pressure the sample is allowed to saturate by being exposed to water filling the top part of cylinder A. The vertical swelling is measured during saturation by the dial gage until com-

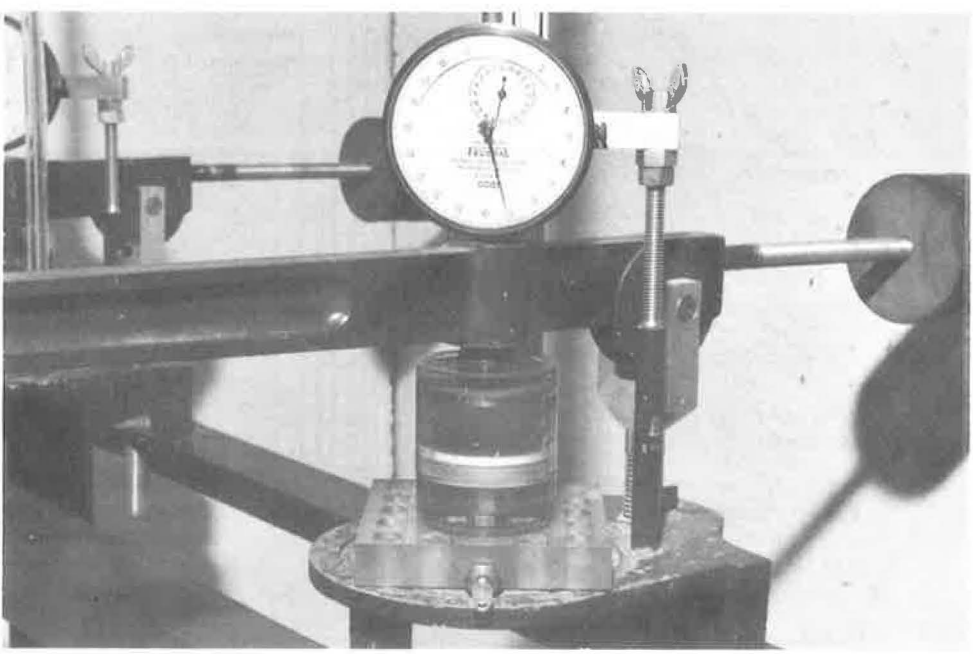

Figure 2. Closeup of tensiometer.

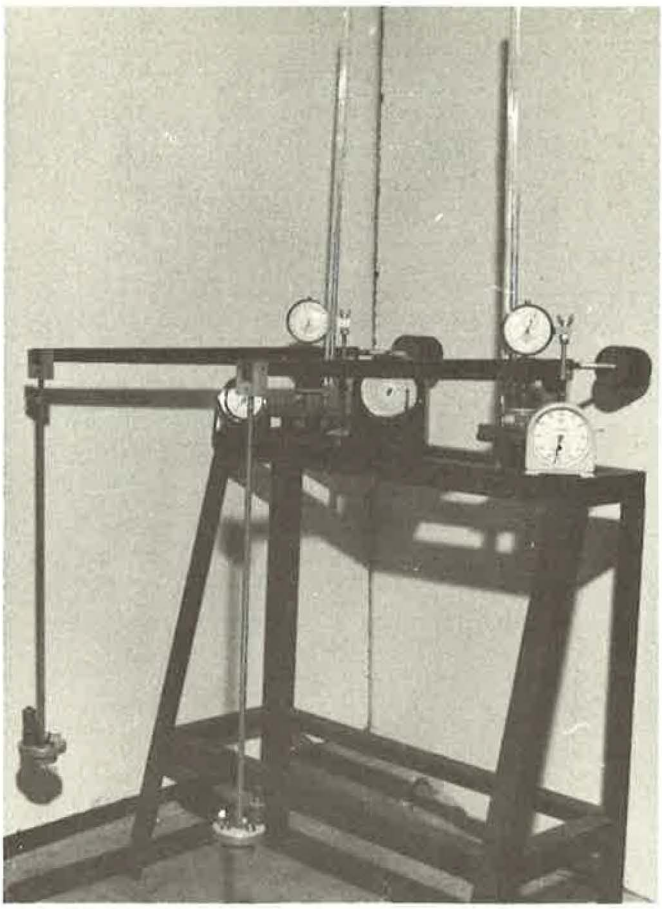

Figure 3. Loading setup of tensiometer for application of external loads.

plete saturation is achieved and no movement is registered, which takes about 7 days. Free water left on top of the sample is then removed and the apparatus is weighed by a precision balance. With the dry weight of the sample and the weight of the apparatus filled with water known, the moisture content at saturation may be determined. The reading on the manometer taken at this stage corresponds to zero suction.

The soil sample is then allowed to dry to the atmosphere. At various stages of the drying process, readings are taken on the manometer to determine the suction and on the dial gage which indicates skrinkage by its downward movement. The corresponding weights of the apparatus at these stages indicate the loss of water, which is used to determine moisture content. Before each weighing, the sample is prevented from drying for 2 to 3 hr to insure moisture equilibrium within the soil.

When the maximum suction measurable by the apparatus is attained ($^3/_4$ atmos), the sample is gradually wetted and the hysteresis in the moisture-suction function is established.

Two corrections should be applied to the weight of the apparatus to allow for the following changes during the process of drying: (a) a correction for the change in the weight of the water within the capillary tube of the manometer due to changes in suction; and (b) a correction for a change in weight of the water within the stand-tube, F, due to accumulation of air, usually occurring at suctions above $^3/_4$ atmos. The weight of the suction plate is assumed constant throughout the test.

| Initial Conditions of Clay | (A) zero press. | (B) 0.15 kg/cm² |
|---|---|---|
| Placement moisture, % | 24.0 | 24.0 |
| Placement Dry Dens. g/cm³ | 1.40 | 1.40 |
| Percent Swell | 12.5 | 6.06 |
| Moisture after Swell, % | 40.5 | 38.3 |

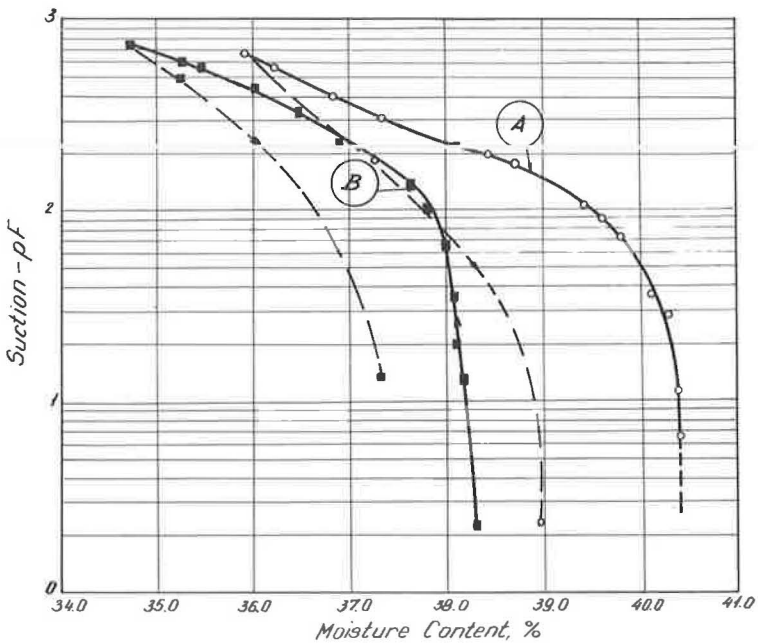


Figure 4. Moisture-suction functions for externally loaded and unloaded heavy clay.

The test is carried out in a constant temperature room to avoid effects of temperature changes on the measurements.

## RESULTS

Two soils were tested by the apparatus, and their moisture-suction functions up to ¾ atmos were determined. The first soil was a heavy clay, with a liquid limit of 75, a plasticity index of 55, and a shrinkage limit of 9.5. The second soil was a uniform fine sand with a 50 percent size equal to 0.15 mm. Both soils were tested for suction under zero external pressure, as well as under an external pressure of 0.15 kg/sq cm.

The test results are shown in Figure 4 for the clay and in Figure 5 for the sand. The difference in suction for the clay (Fig. 4) between the unloaded sample and the loaded one is approximately 0.15 kg/ sq cm, which corresponds to the external pressure on the loaded sample. This means that the compressibility factor, $\alpha$, for this soil is approximately unity, as the clay remained saturated within the range of moistures under which the suction was measured. The corresponding curves for the sand, however, are almost identical (Fig. 5), which means that $\alpha$ is approximately zero, as would be expected from a purely granular soil.

| Initial conditions of Sand | (A) Zero Pressure | (B) 0.15 kg/cm² |
|---|---|---|
| Placement Moisture, % | 12.0 | 12.0 |
| Placement Dry Density, g/cm³ | 1.60 | 1.60 |
| Moisture after Saturation, % | 24.5 | 23.5 |

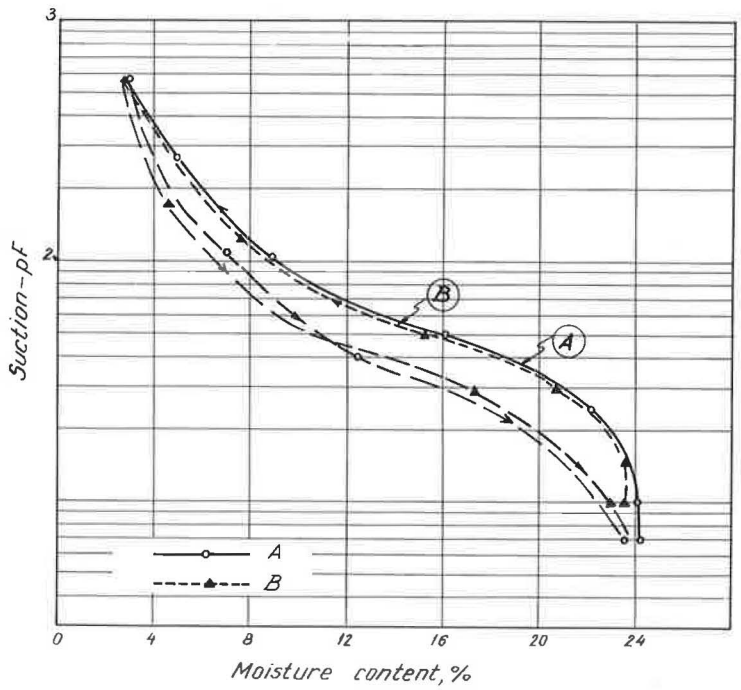


Figure 5. Moisture-suction functions for externally loaded and unloaded sand.

## CONCLUSIONS

An apparatus which measures negative pore pressures during drying and wetting processes under external loads has been described and test results on a heavy clay and a sand presented. As compared with the British methods, the present apparatus has the advantage of continuously measuring suctions under external loads (negative pore pressures) in a single operation. It has also the advantage of determining moisture contents without removing the soil sample from the suction plate, thus avoiding interference in the contact between the soil and the plate. The test results show that for the range of measureable suction the apparatus produced a compressibility factor, $\alpha$, equal to unity for the heavy clay and to approximately zero for the sand, which agrees fully with the RRL work.

The apparatus has, however, the limitation that the range of measureable suctions is up to $^{3}/_{4}$ atmos. Another limitation of the work presented is the small number of soils tested to date. Continuation of this work in respect to both limitations is underway and will be reported in the future.

## REFERENCES

1. Croney, D. and Coleman, J. D. Soil Moisture Suction and Their Bearing on the Moisture Distribution in Soils. 3rd ICSMFE, Zurich, Vol. 1, pp. 13-18, 1953.

2. Black, W. P. M. and Croney, D. Pore Water Pressure and Moisture Content Studies under Experimental Pavements. Proc., 4th ICSMFE London, Vol. 2, pp. 94-99, 1957.
3. Croney D., Coleman J. D., and Black W. P. M. Movement and Distribution of Water in Soil in Relation to Highway Design and Performance. Highway Research Board Spec. Rept. 40, pp. 226-252, 1958.
4. Penner, E. Discussion and Review of Symposium Papers on Water and Its Conduction in Soils. Highway Research Board Bull. 287, pp. 2-6, 1961.
5. Croney, D., and Coleman, J. D. Pore Pressure and Suction in Soil. Proc., Conf. on Pore Pressure and Suction in Soils, Butterworths, London, pp. 31-37, 1961.
6. Globinsky, Z. Model Studies of Suction, Moisture and Movement Variations in Clay Shoulders of Runways. Israel Inst. of Tech. M. Sc. thesis, Technion, Haifa, Israel, 1964.

# A New Equation for Electroosmotic Flow and Its Implications for Porous Media

MELVIN I. ESRIG and STEVEN MAJTENYI
Respectively, Assistant Professor of Civil Engineering and Graduate Research Assistant, Cornell University

A new form of the equation for electroosmotic flow in capillaries has been developed. The equation appears to unify the Helmholtz-Smoluchowski theory, applying to large capillaries with double layers that are thin when compared with the capillary radius, and the Schmid theory, applying to microporous systems with essentially uniform charge distributions. The major advantages of the new equation are simplicity and ability to be used for a wide range of capillary diameters. Analysis of the equation suggests that the electroosmotic velocity of flow in a porous medium such as soil is related to permeability, porosity, pore ion conductivity and soil plasticity properties.

•UNDER the influence of an applied electric field, water will migrate through porous media. Termed electroosmosis, this phenomenon has proven useful in the solution of many engineering problems.

At present only relatively simple theories are available for use in predicting the velocity of water flow during electroosmosis. These theories are mainly based on experiments performed in individual capillary tubes and ignore many important but complicating effects such as those resulting from temperature, ion exchange, and electrolysis as a function of time, surface conductance, nonuniform geometry of capillaries, variable viscosity of the pore fluids, etc. Nevertheless, these theories have proven useful to engineers and scientists.

The discovery of the phenomenon of electroosmosis is credited to Reuss in 1808. Helmholtz (2) proposed the first analytical theory to explain electroosmosis in 1879 and this theory was partially generalized and improved by Smoluchowski (8) in 1921. The Helmholtz-Smoluchowski theory is now considered valid for large capillaries in which the electric double layer is small when compared with the capillary radius. To explain electroosmosis in the special case of very small capillaries (microcapillaries), a theory was presented by Schmid (7) in a series of papers between 1950 and 1952. An attempt to unify the Helmholtz-Smoluchowski and Schmid theories was made by Oel (5) in 1955; however, his equation cannot be integrated when the general case is considered.

The theories of electroosmotic flow are generally referenced to the zeta potential, defined by van Olphen (9) as the "electric potential in the double layer at the interface between a particle which moves in an electric field and the surrounding liquid." It can also be defined as the potential across an equivalent condenser having one plate at the plane of shear in the fluid surrounding the particle and the other some distance away in the mobile part of the electric double layer. A more specific definition of the distance between the plates of the equivalent condenser would be useful in defining electrokinetic phenomena.

This paper presents a simple equation which appears to unify the Helmholtz-Smoluchowski and Schmid theories, defines with precision the distance between the plates of the equivalent condenser and, hopefully, provides a better basis for a physical understanding of the phenomenon of electroosmosis in porous media.

Paper sponsored by Committee on Physico-Chemical Phenomena in Soils.

## NOTATION

$A$ = cross-sectional area of porous medium,
$A_1$ = concentration of wall charges expressed in ionic equivalents per unit volume of pore fluid (number of charges per volume),
$a$ = cross-sectional area of capillary tube,
$C$ = capacity of condenser,
$C_s$ = shape factor,

$d$ = parameter to characterize electric double layer,
$E$ = applied electric field (potential gradient),
$F$ = average electrical driving force per unit volume of electrolyte in capillary,
$F_1$ = 1 faraday (96,490 coulombs),

$k$ = hydraulic permeability of porous medium,
$k_e$ = electroosmotic permeability of porous medium,

$L$ = length,

$\bar{L}$ = length of capillary tube,
$M$ = mass,
$m$ = number of capillaries per unit area of porous material,
$m_n$ = number of capillaries per unit area of porous material with radius $R_n$,

$n$ = porosity (also used for summation index),
$Q$ = quantity of fluid discharged per unit time,

$\bar{Q}$ = electric charge,
$q$ = flow volume per second through individual capillary,
$R$ = effective radius of capillary,
$R_n$ = effective radius of specific capillary,

$r$ = radial coordinate in capillary,
$dr$ = differential radial distance,

$\bar{r}$ = radial distance to circle of electrical gravitation,
$T$ = time,
$t$ = shear stress in fluid,
$v_s$ = velocity of first moving layer (slip velocity),

$V$ = average velocity of water migration in steady-state condition,
$dv$ = differential change in velocity,
$x_s$ = x coordinate of surface of immobile portion of electric double layer,
$x, y, z$ = rectangular coordinates,
$\epsilon$ = dielectric constant of fluid,
$\gamma$ = fluid mass density,
$\pi$ = 3.1416...,
$\pi_n$ = pi product,

$\rho$ = mobile excess electric charge density,

$\bar{\rho}$ = average mobile excess electric charge density,
$\sigma$ = surface charge density,
$\tau$ = thickness of immobile portion of double layer,
$\mu$ = fluid viscosity,
$\zeta$ = zeta or electrokinetic potential, and
$d\theta$ = differential angle in polar coordinate system.

## VARIABLES CHARACTERISTIC OF ELECTROOSMOTIC FLOW

It will be convenient to relate the variables characteristic of electroosmotic flow by use of dimensional analysis. The only restriction placed on this analysis is that a complete set of variables must be chosen which completely define a physical system. Within this limitation, variables may be chosen a priori. If only the balance between viscous and electric forces at steady-state conditions is considered and all complicating effects

discussed previously are ignored, the variables affecting electroosmotic flow can be simply delineated.

The shear stress, t, at any surface element in the capillary is proportional to the rate of change of velocity across the element dv/dr. The constant of proportionality is the coefficient of viscosity, $\mu$, of the fluid. Thus,

$$t = \mu \frac{dv}{dr} \tag{1}$$

This equation implies that the shearing resistance to electroosmotic flow is related to a surface area of shear, a thickness of the shear zone, a velocity, and a coefficient of viscosity. If only electroosmotic flow in a uniform capillary tube is considered, it is reasonable to characterize the surface area by the variable R, the radius of the capillary; the shear zone by d, the characteristic distance of the mobile part of the double layer; the velocity by V, the average velocity of flow in a steady-state condition; and the viscosity by $\mu$, the coefficient of viscosity of the fluid.

The electric driving force is a function of the electric field and the charge. Consequently, the variables E, the applied field (or potential gradient), and $\bar{\rho}$, the average excess mobile charge density, are introduced. (The characteristic volume has the same variable R introduced previously.) The point of application of both the electric and viscous forces is at the distance d from the surface of the immobile layer on the wall of the capillary. This is the same distance d introduced previously and it is discussed in considerable detail subsequently. At this point, however, d may most simply be considered a distance characterizing the electric double layer.

It is also convenient to introduce as a variable $\gamma$, defined as the mass density of the fluid in the capillary. This variable aids in the analysis and disappears from the final form of the expression developed.

Development of Relationship Among Variables

The variables necessary to characterize electroosmotic flow through a capillary tube under the influence of an applied electric field have been developed in the preceding section. They have the fundamental dimensions of mass (M), length (L), time (T), and charge ($\bar{Q}$), as follows:

$\mu$ = coefficient of fluid viscosity, $M\ L^{-1}\ T^{-1}$;

$\gamma$ = fluid mass density, $M\ L^{-3}$;
R = effective capillary radius, L;

V = average velocity of water migration in steady-state condition, $L\ T^{-1}$;
d = distance to characterize electric double layer, L;
$\bar{\rho}$ = average mobile charge density, $\bar{Q}\ L^{-3}$; and

E = applied electric field (or potential gradient), $M\ L\ T^{-2}\ \bar{Q}^{-1}$.

All other variables that might affect electroosmotic flow, such as temperature, time, surface conductance, nonuniform geometry of pores, heterogeneity of material, variable viscosity of pore fluid, electrolysis and possible ion exchange, are not considered further, and the system is assumed to be characterized completely by the seven variables. These assumptions are identical to those made in the development of the Helmholtz-Smoluchowski and Schmid equations. Consequently, the equations developed using them are subject to the same limitations as the Helmholtz-Smoluchowski and Schmid equations.

By applying the Buckingham pi theorem, a mathematical technique to reduce the number of variables of a system to a smaller number of dimensionless parameters that characterize it, three dimensionless parameters may be developed. They are obtained by considering the following three pi products:

$$\pi_1 = f_1(E, V, R, \bar{\rho}\ \gamma) \tag{2a}$$

$$\pi_2 = f_2(d, V, R, \bar{\rho}, \gamma) \tag{2b}$$

$$\pi_3 = f_3(\mu, V, R, \bar{\rho}, \gamma) \tag{2c}$$

Completing the analysis of these pi products, we arrive at the following dimensionless parameters:

$$\pi_1 = \frac{R\rho E}{V^2\gamma} \tag{3a}$$

$$\pi_2 = \frac{d}{R} \tag{3b}$$

$$\pi_3 = \frac{VR\gamma}{\mu} \tag{3c}$$

However, $\bar{\rho}E$ (Eq. 3a) is equal to the average electrical driving force per unit volume of electrolyte in the capillary and can be denoted as F. Thus, if the variables selected for the analysis truly represent the behavior of the system, electroosmotic flow is completely defined as a function of three dimensionless parameters by the following equation:

$$f\left(\frac{RF}{V^2\gamma}, \frac{d}{R}, \frac{VR\gamma}{\mu}\right) = 0 \tag{4}$$

The relationship among the variables in Eq. 4 must be valid for both the Helmholtz-Smoluchowski and Schmid conditions since no assumptions have, as yet, been made limiting the interval in which it is applicable. To develop the relationship among the dimensionless variables, several assumptions must now be introduced.

Lomize et al. (4) argued that the flow through capillaries in an electric field was laminar and similar to hydraulic flow through pipes. Consequently, they reasoned that the product of $\pi_1$ and $\pi_3$, which represent the friction factor and Reynolds number characteristic of hydraulic flow, must be equal to some dimensionless factor of proportionality that is a function of the physical and chemical properties of the system. They showed that this assumption was reasonable and productive but did not define the proportionality factor further.

If it is assumed that the proportionality factor is given by a function of $\pi_2$, the relationship among the dimensionless parameters may be written as:

$$\left(\frac{RF}{V^2\gamma}\right)\left(\frac{VR\gamma}{\mu}\right) = f_4\left(\frac{d}{R}\right) \tag{5}$$

or

$$V = \frac{R^2F}{\mu} f_5\left(\frac{d}{R}\right) \tag{6}$$

To proceed further, it is necessary to define the distance d and to relate it to the zeta potential. Since d is meant to characterize the mobile portion of the electric double layer from both the electrostatic and fluid mechanical point of view, it may be defined as the distance between the center of electrical gravitation of the mobile portion of the double layer and the surface of the immobile portion of the double layer. This definition is indicated for a segment of a capillary tube or for a flat plate in Figure 1a. (Detailed investigation of the final equation using existing double-layer theories has shown that the definition of d is valid.)

When the double layer is contained within a circular capillary tube, the locus of all points defining the center of electrical gravitation of the mobile portion of the double layer will lie on a circle, as shown in Figure 1b, which can be called the circle of electrical gravitation. It may be found by noting that the moment of mobile charges on one side is equal to the moment of charges on the other side. Thus,

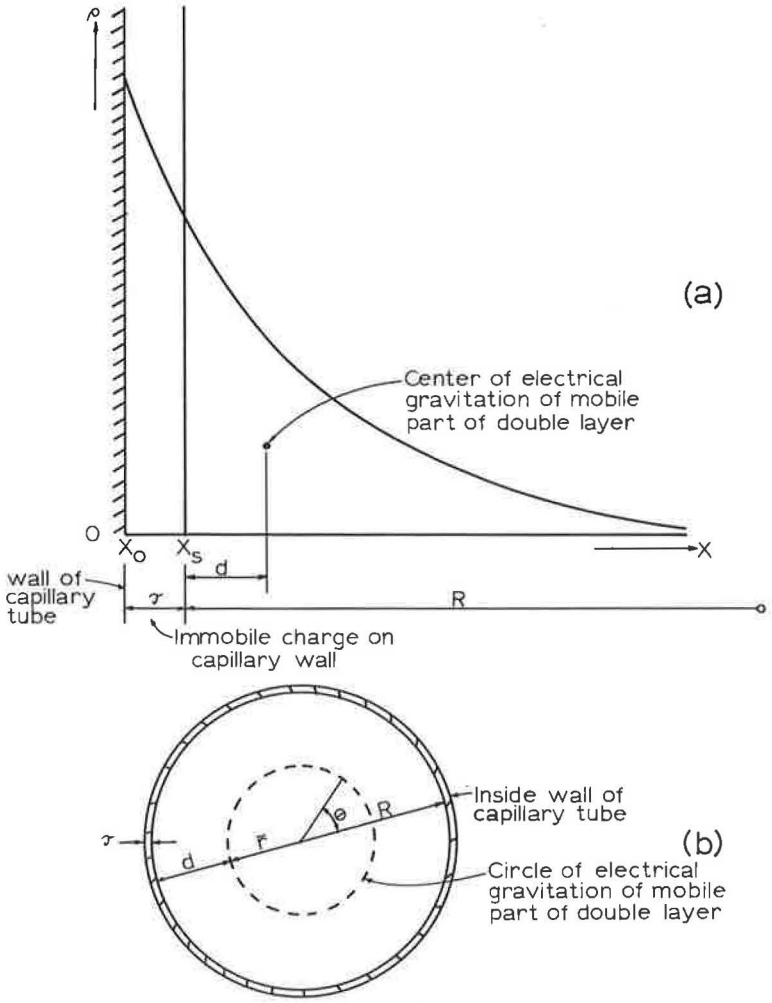


Figure 1. Definition of variables of electric double layer.

$$\underset{\text{inside circle}}{\iint} \rho(\bar{r} - r) \cdot r \cdot dr \cdot d\theta = \underset{\text{outside ring}}{\iint} \rho(r - \bar{r}) \cdot r \cdot dr \cdot d\theta \qquad (7a)$$

where $\bar{r}$ denotes the distance from the center of the capillary tube to the circle of electrical gravitation.

When the thickness of the double layer is small in comparison to the radius of the capillary and, as a result, there is effectively zero excess charge at the center of the capillary, Eq. 7a can be reduced to the simple form:

$$d = \frac{\int_{x_s}^{\infty} \rho \cdot x \cdot dx}{\int_{x_s}^{\infty} \rho \, dx} - x_s \tag{7b}$$

For a circular capillary the distance d may be further defined (Fig. 1b) as:

$$d = R - \bar{r} \tag{8}$$

Then by transforming the Helmholtz-Smoluchowski equation, a first approximation to the function $f_5\left(\frac{d}{R}\right)$ may be obtained.

The Helmholtz-Smoluchowski equation, in the cgs electrostatic system, may be written as:

$$V = \frac{\zeta \epsilon E}{4\pi\mu} \tag{9}$$

where $\zeta$ denotes the zeta or electrokinetic potential, $\epsilon$ denotes the dielectric constant of the capillary fluid, and all other terms have been previously defined. The Helmholtz-Smoluchowski equation is, by virtue of the original assumptions made in its derivation, only valid for the large capillary and the thin double layer.

As a result of the presence of the electric double layer, a cylindrical condenser can be assumed to exist at the walls of the capillary. This is the assumption made by Helmholtz in his original derivation. The capacity, C, of the condenser is given by

$$C = \frac{\epsilon \bar{L}}{2 \log_e \frac{R}{\bar{r}}} \tag{10}$$

where $\bar{L}$ is the length of the capillary tube and all other terms are as previously defined.

The zeta potential, $\zeta$, is the electric potential across the equivalent condenser and must, therefore, charge, $\bar{Q}$, divided by the capacity of the condenser:

$$\zeta = \frac{\bar{Q}}{C} \tag{11}$$

The ratio $R/\bar{r}$ can be transformed in the following manner:

$$\frac{R}{\bar{r}} = \frac{\bar{r} - \bar{r} + R}{\bar{r}} = 1 + \frac{R - \bar{r}}{\bar{r}} = 1 + \frac{d}{\bar{r}}$$

which, for the Helmholtz-Smoluchowski assumptions, is approximately equal to:

$$\frac{R}{\bar{r}} \neq 1 + \frac{d}{R} \tag{12}$$

By substituting Eqs. 10 and 12 into Eq. 11 and noting that the average electric charge per unit volume $\overline{\rho}$ may be given as:

$$\overline{\rho} = \frac{\overline{Q}}{\pi R^2 \overline{L}}$$

it is found that

$$\zeta = \frac{2\pi \overline{\rho} R^2 \log_e \left(1 + \frac{d}{R}\right)}{\epsilon} \tag{13}$$

Eq. 13 shows a relationship between d and the zeta potential. By now substituting Eq. 13 into Eq. 9 we find that:

$$V = \frac{1}{2} \log_e \left(1 + \frac{d}{R}\right) \frac{R^2 F}{\mu} \tag{14}$$

in which F is, as stated previously, $\overline{\rho} E$ or average electrical driving force per unit volume of electrolyte in the capillary. It is also important to note that R refers to the effective radius of the capillary, which is defined as the radius through which flow takes place.

Eq. 14 is in the form of Eq. 6 where:

$$f_5\left(\frac{d}{R}\right) = \frac{1}{2} \log_e \left(1 + \frac{d}{R}\right) \tag{15}$$

Consequently, an equation has been developed for circular capillaries which contains:

1. All the variables required to satisfy the results of the dimensional analysis (Eq. 4),
2. These same variables in a relationship compatible with the assumptions that have been made, and
3. A first approximation of the missing function $f_5\left(\frac{d}{R}\right)$.

Since Eq. 14 has been developed from a transformation of the Helmhotz-Smoluchowski equation, it apparently satisfies the requirements of that theory. It now remains to show that Eq. 14 satisfies the requirements of the Schmid theory.

Development of Schmid-Poiseuille Equation

The Schmid theory was developed for microporous systems in which the charge in the pore fluid can be considered uniformly distributed. Schmid considered his theory valid for capillaries with radii of less than about 500 Å. By following the method of derivation of the Schmid-Poiseuille equation outlined by Winterkorn (10, 11), and introducing into the Poiseuille equation for flow through a capillary tube having a parabolic velocity distribution (no slip at walls) the electric force per unit volume P where

$$P = A_1 F_1 E \tag{16}$$

the following equation results:

$$q = \frac{\pi R^4 A_1 F_1 E}{8\mu} \tag{17}$$

where

q = the flow volume per second,
$A_1$ = concentration of wall charges expressed in ionic equivalents per unit volume of pore fluid (number of charges per volume),

E = electric potential gradient, and
$F_1$ = 1 faraday (96,490 coulombs).

However, the average velocity, V, of the water flowing through the capillary is equal to q/a where a is the area of the capillary cross-section. Thus, the average velocity is equal to:

$$V = \frac{1}{8} \frac{A_1 F_1 E R^2}{\mu} \tag{18}$$

Since the force function, $P = A_1 F_1 E$, is the electric force per unit volume of electrolyte in the capillary and has been designated previously as F, Eq. 18 can be rewritten as:

$$V = \frac{1}{8} \frac{R^2 F}{\mu} \tag{19a}$$

Once again the dimension R, appearing in Eq. 19a, refers to the effective radius of the capillary through which fluid flows. No fluid can flow through the zone occupied by the immobile layer on the capillary wall. Since by definition the dimension R is entirely within the mobile portion of the electric double layer (Fig. 1a), movement of fluid must be expected over the entire effective width of the capillary. As a consequence, slip must occur at the distance R from the center of the capillary tube and Eq. 19a, which has been derived assuming no slip conditions, should predict an average velocity that is too small.

If the general form of the Poiseuille equation is solved using the Schmid force function (Eq. 16), and assuming that slip occurs and the velocity of the first moving layer is given by $v_S$, the average velocity, V, is

$$V = v_S + \frac{1}{8} \frac{R^2 F}{\mu} \tag{19b}$$

It can be concluded, therefore, that the use of Eq. 19a is likely to predict a minimum average velocity of electroosmotic flow for microporous systems.

Eqs. 14 and 19a can be shown to be essentially the same, and a first indication is obtained that Eq. 14 may be a general form of the equation for electroosmotic flow if the factor $\frac{1}{2} \log_e \left(1 + \frac{d}{R}\right)$ is nearly equal to 1/8 when the Schmid conditions are imposed on the analysis. For these conditions in a circular capillary, the charge density $\rho$ is a constant and the moment of charge on one side of the circle of electrical gravitation (Fig. 1b) must be equal to the moment of charge on the other side. Therefore, from Eq. 7:

$$\int_0^{\bar{r}} (\bar{r} - r) \cdot r \cdot dr = \int_{\bar{r}}^{R} (r - \bar{r}) \cdot r \cdot dr \tag{20}$$

Integrating Eq. 20 and rearranging terms leads to the following:

$$\frac{d}{R} = \frac{1}{3} \tag{21}$$

Substituting d/R = 1/3 into Eq. 15 produces a factor $\frac{1}{2} \log_e \left(1 + \frac{d}{R}\right)$ equal to 0.144. This value exceeds 1/8 by about 15 percent, which is considered a reasonable check of Eq. 19a. Part of the difference results from the fact that Eq. 15 represents only a

first approximation to the missing function $f_5\left(\frac{d}{R}\right)$. Additional difference results from the assumption, for both the Helmholtz-Smoluchowski and Schmid conditions, that the slip velocity is zero. Recent work has shown that any slip velocity other than zero will have a relatively more important effect on the average velocity when small, rather than large, capillaries are considered.

It appears from the preceding discussion that a simple expression has been developed for circular capillaries which unifies, within reasonable limits, the Helmholtz-Smoluchowski and Schmid equations. This expression has the advantage of treating a range of capillary diameters and can be used together with existing double-layer theories to predict velocities under a wide range of conditions. Recent work has shown that Eq. 14 is entirely compatible with the double-layer theories presented by Bolt (1). Eq. 14 also leads to some interesting conclusions with regard to electroosmotic flow through porous media.

Implications for Porous Media

The average velocity of flow of water in a single capillary subjected to an electric field may now be approximated by Eq. 14. The total quantity of flow per unit time, q, through this capillary is given by:

$$q = \frac{\pi R^4 \bar{\rho} E}{2\mu} \log_e \left(1 + \frac{d}{R}\right) \tag{22}$$

where $\bar{\rho}E$ has been substituted for F.

It is apparent that the flow through the capillary is dependent on the capillary radius and that the flow through a group of capillaries of different radii cannot be truly a function of parameters like the average capillary radius or the porosity of the system. However, the error introduced by using these parameters can be shown to be small.

Expanding the logarithmic function in Eq. 14 in the Taylor series and using only the first term, d/R, to represent the entire series introduces into the equation an error that must be smaller than 17 percent. Consequently, the average velocity of flow, overstated by no more than 17 percent, may be represented as:

$$V = \frac{1}{2} \frac{dR \bar{\rho} E}{\mu} \tag{23}$$

Moreover, the average mobile charge density $\bar{\rho}$ is related to a uniform surface charge density by:

$$\bar{\rho} \pi R^2 = (-\sigma)\ 2\pi R \tag{24}$$

or

$$\rho = \frac{2(-\sigma)}{R} \tag{25}$$

where the minus sign indicates a surface charge opposite in sign to that in the mobile portion of the double layer.

By substituting Eq. 25 into Eq. 23, we find that

$$V = \frac{d(-\sigma)E}{\mu} \tag{26}$$

indicating that the average velocity of flow is, for the case of a uniform surface charge density, sensibly independent of radius of the capillary.

The outflow per unit time, q, for the individual capillary is a function of the area of the capillary cross-section:

$$q = a \cdot V \tag{27}$$

where a has previously been defined as the effective area of an individual capillary and is equal to $\pi R^2$. Therefore, for a bundle of $m_n$ capillaries per unit area of radius $R_n$, discharging from a gross area A, the total discharge, Q, may be written as:

$$Q = \sum_{0}^{n} m_n \pi R_n^2 \, A \cdot V \tag{28}$$

However, the term $\sum_{0}^{n} m_n \pi R_n^2$ is exactly equal to the porosity, n, of the system. Thus,

$$Q = nA \cdot V \tag{29}$$

Eq. 26 is only correct to within 17 percent when a uniform charge density exists on the walls of the capillaries, the capillaries are straight, and the electric field is uniform. In a porous medium, such as soil, the charge density cannot usually be assumed to be uniform because of irregularities in the structure of some of the clay minerals and the common occurrence of several clay minerals intermixed with sand and silt grains. Thus, the velocity is most probably a linear function of capillary radius as indicated by Eq. 23. The capillary radius, in turn, may be related to the hydraulic permeability and porosity (3) by:

$$R = \left( C_S \frac{\mu}{\gamma} \frac{k}{n} \right)^{1/2} \tag{30}$$

where $C_S$ denotes a shape factor that takes into account the tortuosity of flow channels in porous media. Substituting Eq. 30 into Eqs. 29 and 23 we find that:

$$Q = C_1 \left( \frac{kn}{\mu\gamma} \right)^{1/2} d \cdot \overline{\rho} \cdot EA \tag{31}$$

where $C_1$ is a constant related to the shape factor. Defining electroosmotic flow in a form analogous to Darcy flow as follows:

$$Q = k_e \cdot E \cdot A \tag{32}$$

where $k_e$ represents an electroosmotic coefficient of permeability and E is the potential gradient, we find that

$$k_e = C_1 \left( \frac{kn}{\mu\gamma} \right)^{1/2} d \cdot \overline{\rho} \tag{33}$$

and $k_e$ is related to the hydraulic permeability and the porosity of the system.

One side advantage of relating electroosmotic flow to hydraulic permeability as done here is that, in the form of Eq. 31, the electroosmotic flow equation includes a correction for the tortuosity of the flow path in the porous media. This correction factor is not exactly correct since $C_1$ is related to $\left( C_S \right)^{1/2}$, and the shape factor for electroosmotic flow may be different from that for hydraulic flow, but it is a convenient step in the proper direction.

Other implications of Eq. 14 are that electroosmotic flow is directly related to double layer thickness which is, in turn, related to pore ion concentration. Thus, electric conductivity measurements should be obtained when attempting to predict the usefulness (and economy) of electrokinetic treatment.

When applied to saturated soils, Eq. 14 implies that the higher the water content of the soil mass, the greater is the electroosmotic flow, except when the soil-water system becomes fluid and the soil particles are able to move. By definition, the fluid state would be expected at water contents in the neighborhood of the liquid limit of the soil. A reduction of the electroosmotic flow has been shown by Piaskowski (6) and Winterkorn (10) to occur at these water contents.

The relationship between surface charge density and velocity of flow leads to the conclusion that the effectiveness of electrokinetic treatment of soils should be related to the plasticity properties of soils since the higher the surface charge density, the higher are the expected Atterberg limits. Consequently, greater effectiveness of electroosmotic treatment would be expected in montmorillonitic soils than in kaolinitic soils.

## CONCLUSIONS

A general equation for electroosmotic flow in circular capillaries appears to have been developed. The new equation has been checked against the Helmholtz-Smoluchowski and Schmid-Poiseuille equations, which are the two limiting cases. Its advantages are that it has a simple form, it can be used with any existing or improved double-layer theories, it permits the prediction of velocities for a wide range of capillary diameters, and it provides better physical insight into the process of electroosmotic flow than most existing theories. It is, however, subject to essentially the same limitations as most equations. Analysis of the new equation suggests that for a porous medium such as soil, the electroosmotic velocity of water flow is related to permeability, porosity, pore ion conductivity and soil plasticity properties. These variables must be investigated in determining the suitability of a soil for electrokinetic treatment.

## ACKNOWLEDGMENTS

The analysis presented in this paper was developed as part of a research investigation, "Feasibility Study of Electrokinetic Processes for Stabilization of Soils for Military Mobility Purposes," conducted for the U. S. Army Engineer Waterways Experiment Station under the sponsorship of the U. S. Army Materiel Command.

The authors are particularly appreciative of the counsel of Professor R. D. Miller of the Agronomy Department of Cornell University and of the opportunity he provided for discussion of this work with Dr. G. H. Bolt.

## REFERENCES

1. Bolt, G. H. The Significance of the Measurement of the Zeta Potential and the Membrane Potential in Soil and Clay Suspensions. M. S. thesis, Cornell Univ., 1952.
2. Helmholtz, H. von. Ann. Physik Wiedemann. Vol. 7, p. 337, 1879.
3. Leonards, G. A. Foundation Engineering. New York, McGraw-Hill, 1962.
4. Lomize, G. M., Netushil, A. V., and Rzhanitzin, B. A. Electroosmotic Processes in Clayey Soils and Dewatering During Excavations. Proc. 4th Int. Conf. on Soil Mech. and Found. Eng., Vol. 1, pp. 62-67, 1957.
5. Oel, H. J. Zur Theorie der Electrokinetischen Ersheinungen. Z. fur Phys. Chem., Neue Folge, Vol. 5, pp. 32-51, 1955.
6. Piaskowski, A. Investigation on Electro-osmotic Flow in Soils in Relation to Different Characteristics. Proc. 4th Int. Conf. on Soil Mech. and Found. Eng., Vol. 1, pp. 89-92, 1957.
7. Schmid, G. Series of papers in Z. Electrochem., Vol. 54, p. 424, 1950; Vol. 55, pp. 229, 684, 1951; Vol. 56, pp. 35, 181, 1952.
8. Smoluchowski, M. von. Handbuch der Electrizitat und des Magnetismus. Vol. 2, p. 366. Leipzig, J. A. Barth, 1921.
9. Van Olphen, H. An Introduction to Clay Colloid Chemistry. N. Y., Interscience, 1963.
10. Winterkorn, H. F. Surface Chemical Properties of Clay Minerals and Soils from Theoretical and Experimental Developments in Electroosmosis. ASTM Sp. Tech. Pub. 142, pp. 44-52, 1952.
11. Winterkorn, H. F. Potentials in Moisture Migration. Bull. No. 1, Div. of Bldg. Res., N. R. C., pp. 86-101, 1955.

## *Discussion*

H. C. LEITCH, Graduate Research Assistant, McGill University, Montreal, Canada— This paper is of considerable interest in that it provides a fresh approach to the problem of establishing the physical significance of the coefficent of electroosmotic permeability. The dimensional analysis used to derive the equation presented here closely parallels that used by Leonards (3) to establish the generalized Hagen-Poiseuille equation for hydraulic flow:

$$V = C_S \left(\frac{\gamma S}{\mu}\right) R_H^2 \tag{34}$$

where

$V$ = superficial hydraulic flow velocity;
$C_S$ = shape factor, introduced to account for the shape of the pore cross-section;
$R_H$ = hydraulic radius;
$\gamma$ = unit weight of fluid;
$S$ = hydraulic gradient; and
$\mu$ = coefficient of absolute viscosity of the fluid.

Thus, it is not surprising that a similar result can be obtained from a modification of Eq. 34. The required modification is achieved by replacing the hydraulic gradient, S, by an equivalent electroosmotic gradient, $S_e$, which may be written as:

$$S_e = f\left\{\frac{E\bar{\rho}}{\gamma}\right\} \tag{35}$$

where

$E$ = applied electric field, and
$\bar{\rho}$ = average excess charge density of mobile portion of diffuse ion layer.

By the use of this substitution, it is possible to write an electroosmotic flow equation of the form

$$V = C_{S_e} \frac{\gamma}{\mu} R^2 \cdot f\left\{\frac{E\bar{\rho}}{\gamma}\right\} \tag{36}$$

where

$V$ = superficial electroosmotic flow velocity,
$C_{S_e}$ = electroosmotic shape factor, and
$R$ = electroosmotic radius, related to the hydraulic radius.

The approximations used in the original presentation allow the evaluation of the electroosmotic gradient, $S_e$, as

$$S_e = f\left\{\frac{E\bar{\rho}}{\gamma}\right\} \cong \frac{d}{R} \cdot \frac{E\bar{\rho}}{\gamma} \tag{37}$$

where d is a parameter introduced to characterize the properties of the diffusion layer (see Fig. 1a). Thus, Eq. 36 becomes:

$$V = C_{S_e} \frac{R}{\mu} d\bar{\rho} E \tag{38}$$

and if

$$Q = nAV \tag{39}$$

where

Q = discharge per unit time,
n = equivalent porosity (based on free volume of pores), and
A = cross-sectional area of soil,

Eq. 39 becomes

$$Q = C_{S_e} \frac{R}{\mu} d\,\bar{\rho}\, n E A \tag{40}$$

If it is further assumed that $R \cong R_H$, a combination of the Hagen-Poiseuille equation with Darcy law yields the relationship:

$$Q = \frac{C_{S_e}}{\sqrt{C_S}} \left\{ \frac{kn}{\mu\gamma} \right\}^{1/2} d\,\bar{\rho}\, E A \tag{41}$$

where k is hydraulic permeability.

Electroosmotic flow has been described (13) by the empirical equation:

$$Q = k_e E A \tag{42}$$

where $K_e$ is electroosmotic permeability. Using this relationship,

$$\text{Constant } C_1 = \frac{C_{S_e}}{\sqrt{C_S}} \tag{43}$$

Therefore, Eq. 41 may be simplified to

$$k_e = C_1 \left\{ \frac{kn}{\mu\gamma} \right\}^{1/2} d\bar{\rho} \tag{44}$$

which is Eq. 33 of the paper under discussion.

It would seem, however, that $C_1$ is related to $(C_S)^{-1/2}$ and, thus, serves to generalize by taking into account, at least partially, any deviation from the circular in the shape of the cross-section of the soil pores. It does not, however, offer any correction for the tortuosity of the flow path within the soil.

From Eqs. 41 and 44 and from Eq. 14 of the paper under discussion, it would seem that the effectiveness of electroosmotic treatment would vary directly with the excess charge of the cations in the mobile portion of the double layer. The high surface charge density and, perhaps more important, the high specific surface associated with montmorillonitic clays would reduce this quantity to below that of a less active kaolinitic soil, all other factors being equal. The reduction in the excess charge of the diffuse ion layer would be at least partially offset by an increase in the parameter d and in the hydraulic permeability, but experimental evidence shows that electroosmotic permeability decreases slightly with increasing activity. Casagrande (13) found that $k_e$ — $2 \times 10^{-5}$ cm/sec for Na bentonite at a water content of 170 percent and $5 \times 10^{-5}$ cm/sec for a less active clayey silt.

The efficiency of electroosmotic dewatering, as opposed to hydraulic dewatering, may be characterized by the ratio $k_e/k$. In the case of the two soils mentioned, $k_e/k$ is $2 \times 10^6$ for the Na bentonite and $6.25 \times 10^2$ for the clayey silt. Thus, even though the electroosmotic permeability of the bentonite was found to be slightly less than that of the clayey silt, its suitability to electroosmotic treatment is considerably greater.

It should also be pointed out that a significant change in outflow under a constant macroscopic electric potential gradient can occur over a period of time, particularly in active soils at high water contents. It would appear that this effect is due largely to

local changes in the resistivity of the soil-water system which lead to changes in the microscopic electric gradient (12).

References

12. Cambefort, H., and Caron, C., Electro-osmose et Consolidation Electro-Chemique des Agriles. Géotechnique, Vol. 11, pp. 203, 1961.
13. Casagrande, L. Electro-osmosis in Soils. Géotechnique, Vol. 1, No. 3, 1949.

M. I. ESRIG and S. MAJTENYI, Closure—Mr. Leitch's discussion raises several important questions about electroosmotic flow of water in soils and about the equations we have developed. These questions are related to the use of the Poiseuille equation in characterizing electroosmotic flow, the effect of the shape and tortuosity of the soil pores on this flow, the physical significance of the new equation we have proposed, and the effects of time on electroosmotic flow.

As Mr. Leitch has suggested, the use of the Poiseuille equation, whether or not it is developed from a dimensional analysis, to characterize electroosmotic flow in capillaries can, under a limited set of circumstances, be correct. Use of this equation is only correct when the driving force is uniform across the cross-section of the capillary. This limitation was recognized by Winterkorn (10, 11) when he developed what we have termed the Schmid-Poiseuille equation that characterizes electroosmotic flow in microcapillaries. However, when the capillary diameter becomes so large that the Helmholtz theory is applicable (d/R is small and approaches a minimum value), the electrical driving force is no longer uniformly distributed but is localized in a small region near the capillary wall. For this condition, the Poiseuille equation is not applicable.

Mr. Leitch's implication, that the introduction of the electroosmotic force function into the Poiseuille equation produces simply and quickly the new equation for electroosmotic flow, obscures the main problem (and contribution) of the paper. That is, a first approximation to the function $f_5\ d/R$ has been developed which unifies the Helmholtz-Smoluchowski and Schmid theories. Using Mr. Leitch's approach, which is an extrapolation of the Poiseuille equation, it is not possible to develop this function.

Mr. Leitch's comments about the correction for shape and tortuosity are correct if the factor $C_S$ is defined in accordance with the development presented by Leonards (3) only as a correction factor to account for the shape of the capillary cross-section. However, it was our intention to define this factor as a combined shape and tortuosity correction, since these corrections are essentially inseparable when determining soil permeabilities. In our opinion, such a definition does not change the analysis presented in the paper. In addition, if it is assumed that the imposition of the electrical field on the soil mass does not alter the shape or tortuosity of the capillaries (an assumption that may be subject to some question) it is apparent from Eq. 41 that $C_1 = C_S{}^{1}/_{2}$. Since $C_S$ must be less than unity, it is also readily seen that $C_1$ is closely equal to unity for a wide range of values of $C_S$. Thus, in the form of Eq. 31, the coefficient $C_1$ can probably be assumed equal to unity with a loss in accuracy which is small in comparison to the many other uncertainties present when one tries to predict electroosmotic flows.

Mr. Leitch has also pointed out the rather important interrelation of the parameters d and $\bar{\rho}$. He has argued that the product of d and $\bar{\rho}$ should increase with soil activity and that the electroosmotic permeability of the soil should, therefore, increase. He points out, however, that increasing the activity of a soil from that of a clayey silt to a bentonite has been shown to decrease $k_e$. We are in agreement with Mr. Leitch's analysis and have experimental evidence to suggest that it is correct but that he has not carried it quite far enough. For example, referring to Eq. 31, which is only a simplification of Eq. 14 into which the relevant engineering index properties of soil have been introduced, it is apparent that the net effect of a reduction in the permeability of soil from that of the clayey silt ( $8 \times 10^{-8}$ cm/sec) to that of the bentonite ($1 \times 10^{-11}$

cm/sec) would be a decrease in $k_e$. A further decrease could be expected because the pore fluid conductivity of the sodium bentonite was reported to be 5 times greater than that of the clayey silt, tending to decrease the parameter d significantly. Complicating this sort of qualitative analysis is the fact that in bentonite a reduction in electroosmotic outflow would be expected as a result of the presence of positive charges on the edges of the particles while negative charges are present on the faces. Consideration of these factors, together with those indicated by Mr. Leitch, leads to the conclusion that qualitative evaluation of our equation predicts changes in $k_e$ in agreement with experimental evidence.

Finally, we have specifically excluded from our analysis the effects of time on the electroosmotic permeability of soils. It is recognized that physical and chemical changes occur with time in soils subjected to an electric field. These changes will change the electroosmotic permeability of the soil, generally tending to decrease it. We only intend that our analysis be considered applicable for a very short period after an electric field is applied.